A CHEMICAL AND THERMODYNAMIC MODEL OF ALUMINOUS DIOCTAHEDRAL 2:1 LAYER CLAY MINERALS IN DIAGENETIC PROCESSES: REGULAR SOLUTION REPRESENTATION OF INTERLAYER DEHYDRATION IN SMECTITE

BARBARA RANSOM* AND HAROLD C. HELGESON**

ABSTRACT. Consideration of experimental data reported in the literature indicates that dioctahedral aluminous smectite can be regarded as a regular solid solution of hydrous and anhydrous thermodynamic components that differ in stoichiometry only by 4.5 moles of H_2O in the interlayer position (per $O_{10}(OH)_2$).[1] All H_2O that may be present in the smectite interlayer in excess of 4.5 moles is considered to have the properties of bulk water. Equilibrium constants (K) and regular solution Margules parameters (W_s) for the dehydration of Na- and Ca-smectite at 25°C and 1 bar were generated from vapor-pressure isotherm data reported by Keren and Shainberg (1975). The calculations were carried out assuming the stoichiometric number of moles of interlayer H_2O in the smectite components to be independent of the composition of the 2:1 silicate layer, as well as the number and identity of the interlayer cations. The thermodynamic calculations resulted in values of log K and W_s of -3.61 and -2883 cal/mol, respectively, for Ca-smectite and -0.767 and -3254 cal/mol, respectively, for Na-smectite. These values, together with the electrostatic properties of the interlayer cations were used to estimate values of log K and W_s for the dehydration of K-, NH_4-, Rb-, Cs-, Mg-, Sr-, and Ba-smectite. Equilibrium hydration states at 25°C and 1 bar predicted from the estimated values of log K and W_s are in close agreement with those reported in the literature. This observation strongly supports the general validity of describing smectite dehydration in terms of regular solution theory, which requires random mixing of the hydrous and anhydrous components of the minerals. Because the hydration states of smectite predicted in the present study are in close agreement with those inferred from XRD patterns of natural clay samples, the hydrous and anhydrous components of smectite may well correspond to hydrous and anhydrous layers in the mineral. Under these circumstances, smectites in partial states of dehydration should generate diffractograms similar to those of randomly interstratified mixed-layer clays. In the case of

* Scripps Institution of Oceanography, GRD 0220, University of California at San Diego, La Jolla, California 92093.
** Department of Geology and Geophysics, University of California, Berkeley, California 94720.

---

[1] The term component is used in the present communication in its strict thermodynamic sense. A thermodynamic component of a mineral corresponds to a chemical formula unit representing one of the minimum number of independent variables required to describe the composition of the mineral. All stoichiometric minerals are thus composed of a single component corresponding to the formula of the mineral. However, because the term component does not necessarily have any physical connotation, the minerals themselves are *not* components. The terms hydrous and anhydrous components are used to distinguish between chemical units with and without 4.5 moles of interlayer H_2O per $O_{10}(OH)_2$ (see below). Similarly, the term dehydration is used to refer to replacement of hydrous smectite interlayers by their anhydrous counterparts.

K-saturated smectites, the XRD patterns would be identical to those commonly ascribed to randomly interstratified illite/smectite, despite the fact that no layers of illitic composition are present in the mineral.

INTRODUCTION

The behavior and thermodynamic properties of interlayer H_2O in dioctahedral aluminous smectites at 25°C and 1 bar have been the subject of many studies (Barshad, 1955, 1960; Mooney, Keenan, and Wood, 1952; Greene-Kelley, 1962; Martin, 1962; Fripiat and others, 1965; Roderick, Senich, and Demirel, 1969; Keren and Shainberg, 1975, 1979, 1980; Tardy and others, 1980; Omerod and Newman, 1983; Tardy and Touret, 1987; Kraehenbuehl and others, 1987; Tardy and Duplay, 1992; and others). However, the values of thermodynamic properties retrieved from these investigations commonly differ substantially from one another. The differences arise from factors such as the extent to which the various clay mineral samples were monomineralic, the relative amount of interlayer H_2O taken up by the various samples compared to that adsorbed in pores and on particle surfaces, failure to reverse vapor-pressure isotherm experiments, inadequate provision for the effects of different interlayer cations on dehydration, and undocumented factors such as grain shape, surface area, and pore structure. Nevertheless, the samples used in a few of the experimental studies were sufficiently well-characterized to be definitive with respect to changes in the hydration state of smectite interlayers with increasing or decreasing activity of H_2O at 25°C and 1 bar. One of the more comprehensive and internally consistent of these is the study reported by Keren and Shainberg (1975). The purpose of the present communication is to report the results of a thermodynamic analysis of Keren and Shainberg's (1975) data, which permit generation of a provisional frame of reference for describing the chemical and thermodynamic behavior of smectite dehydration (see footnote 1) in diagenetic process (Ransom and Helgeson, 1994a, b).

Just as H_2O in the channels of zeolites is an essential part of zeolite stoichiometry, interlayer H_2O is an integral part of smectite. However, interlayer H_2O is rarely included explicitly in smectite stoichiometries, and none of the existing additivity algorithms for estimating the Gibbs free energy of smectite includes provision for the thermodynamic contribution of interlayer H_2O to the mineral (Tardy and Garrels, 1974; Nriagu, 1975; Mattigod and Sposito, 1978; Chermak and Rimstidt, 1989). As a result, differences between the thermodynamic properties of interlayer H_2O and bulk H_2O are not taken into account, either implicitly or explicitly, when such estimates are used to calculate the thermodynamic properties of reactions involving smectite. As emphasized by Tardy and Duplay (1992), failure to include explicit provision for interlayer H_2O in chemical reactions involving smectite precludes retrieval of accurate thermodynamic properties of smectite from experimentally determined properties of such reactions. Errors of this kind can be avoided by assessing the thermodynamic properties of interlayer H_2O in smectite and including explicitly interlayer H_2O as part of the structural .

formula of the solid solution in a manner similar to that adopted for zeolites. The generalized structural formula for one mole of a smectite solid solution based on a half unit cell (that is, $O_{10}(OH)_2$) can then be expressed as

$$A_i(R_x^{3+}R_y^{2+})_q(Al_zSi_{4-z})O_{10}(OH)_2 \cdot n_{il}H_2O \qquad (1)$$

where A is a proxy for the interlayer cation, R^{3+} and R^{2+} represent trivalent and divalent cations, respectively, the subscripts i, x, y, and z designate the number of moles of the respective cations per half unit cell in the various structural sites, q stands for the number of occupied octahedral sites per mole of the mineral, and n_{il} denotes the number of moles of interlayer H_2O in the smectite formula. These symbols, together with the others used in the following pages are listed in the Glossary.

<div align="center">GLOSSARY OF SYMBOLS</div>

a	The a crystallographic dimension in the monoclinic crystal system.
a_{as}, a_{hs}	Activity of the anhydrous and hydrous components, respectively, of smectite solid solutions.
a_{H_2O}	Activity of H_2O in the liquid state.
a_1, a_2	Cation- and charge-independent parameters used to estimate the equilibrium constant for smectite dehydration (eq 21).
as	Symbolic anhydrous component of smectite solid solutions.
A	Cation occupying the interlayer sites in smectite.
b	The b crystallographic dimension in the monoclinic crystal system.
b_1, b_2	Cation- and charge-independent parameters used to estimate Margules parameters for binary solid solutions of hydrous and anhydrous smectite components (eq 22).
c	The c crystallographic dimension in the monoclinic crystal system.
$f_{H_2O}, f_{H_2O}^\circ$	Fugacity and standard state fugacity, respectively, of H_2O.
g_k, g_s	Grams of H_2O taken up by a kaolinite or smectite sample, respectively, per gram of dried clay (eq 16).
G_{xs}	Excess molal Gibbs free energy of a binary regular solid solution (eq 9).
$\Delta G_{f,H_2O(g)}^\circ,$ $\Delta G_{f,H_2O}^\circ$	Standard molal Gibbs free energy of formation from the elements of steam and water, respectively.
ΔG_j°	Standard molal Gibbs free energy of solvation of the jth cation (eq 19).
ΔG_r°	Standard molal Gibbs free energy of reaction.

$\Delta G^{\circ}_{r,P_r,T_r}$ Standard molal Gibbs free energy of reaction at the reference pressure (P_r) and temperature (T_r) of 1 bar and 298.15 K.

hs Symbolic hydrous component of smectite solid solutions.

$H_2O_{(g)}$ H_2O vapor.

i Number of moles of interlayer cations in one mole of smectite.

j Index for cations in bulk solution or in the interlayers of smectite.

K Equilibrium constant.

M_s, M_w Molecular weight of smectite and H_2O, respectively.

n_c Stoichiometric number of moles of interlayer H_2O in one mole of the hydrated smectite component (that is, 4.5) (eq 15).

n_{il} Number of moles of interlayer H_2O in one mole of a smectite solid solution (eqs 1 and 16).

N_0 Avogadro's number (6.023×10^{23} atoms/mol).

$p_{H_2O}, p^{\circ}_{H_2O}$ Partial pressure of H_2O in the vapor phase and the partial pressure of H_2O corresponding to that of the equilibrium solubility of H_2O in the vapor phase, respectively, at the temperature and pressure of interest.

P_r Reference pressure (1 bar).

q Number of moles of octahedral sites occupied by R^{3+} cations in one mole of smectite.

$r_{e,j}$ Effective electrostatic radius of the jth cation.

R Gas constant (1.9872 cal/mol · K).

R^{2+}, R^{3+} Divalent and trivalent cations, respectively, occupying octahedral sites in smectite 2:1 silicate layers.

T, T_r Temperature in Kelvins and the reference temperature (298.15 K), respectively.

V Vacant interlayer site in smectite (fig. 1).

V_{il} Molal volume of the fully hydrated smectite interlayer (77.5 cm^3 per $O_{10}(OH)_2$).

W_s Margules parameter for a binary regular solid solution of hydrous and anhydrous smectite components (eq 9).

x Number of moles of octahedral R^{3+} cations in one mole of smectite.

X_{as}, X_{hs} Mole fraction of the anhydrous and hydrous component, respectively, of smectite solid solutions.

y Number of moles of octahedral R^{2+} cations in one mole of smectite.

z Number of moles of tetrahedral Al in one mole of smectite.

Z_j Valence of the jth cation.

Z_l Absolute value of the charge on smectite 2:1 silicate layers.

β Angle between the a and c crystallographic directions in the monoclinic crystal system.

χ_{H_2O} Fugacity coefficient of H_2O vapor.

ϵ Dielectric constant of H_2O.

η Dimensional constant in eq (20) (1.66027×10^5 Å cal mole^{-1}).

$\lambda_{as}, \lambda_{hs}$ Activity coefficient of the anhydrous and hydrous component, respectively, of smectite solid solutions.

ω_j Born coefficient of the jth cation.

Φ Regression parameter defined by eq (12).

ρ_{il} Density of interlayer H_2O taken from Hawkins and Egelstaff (1980) (1.05 g/cm^3).

The compositions and thermodynamic behavior of most natural aluminous dioctahedral smectite solid solutions represented by formula (1) can be described in terms of the thermodynamic components (see footnote 1) listed in table 1 for smectites with Na^+, K^+, or Ca^{2+} in the interlayer sites (Ransom and Helgeson, 1993). In contrast to the set of thermodynamic components represented by the oxides K_2O, Na_2O, CaO, MgO, FeO, Al_2O_3, Fe_2O_3, SiO_2, and H_2O, those in table 1 must be both

TABLE 1

Thermodynamic components of smectite solid solutions expressed for the half unit cell represented by $O_{10}(OH)_2$

$KAl_3Si_3O_{10}(OH)_2$

$NaAl_3Si_3O_{10}(OH)_2$

$Ca_{0.5}Al_3Si_3O_{10}(OH)_2$

$K_3Al\ Si_4O_{10}(OH)_2$

$Al_2Si_4O_{10}(OH)_2$

$Fe_2Si_4O_{10}(OH)_2$

$Mg_3Si_4O_{10}(OH)_2$

$Fe_3Si_4O_{10}(OH)_2$

$Na\ Al_3Si_3O_{10}(OH)_2 \cdot 4.5\ H_2O$

added and subtracted to describe the compositions of smectite solid solutions.[2]

The thermodynamic properties of the hydration/dehydration process in smectite are traditionally expressed in terms of mixing H_2O molecules and vacancies on interlayer sites in the mineral. Because the hydration or dehydration of smectite involves solely the addition or loss of interlayer H_2O, the composition of the smectite 2:1 silicate layers across any dehydration reaction remains unchanged. As a result, the silicate layers of the mineral are generally considered to constitute an inert substrate with the interlayer serving as a solvent into which the solute species (H_2O) dissolves (Barshad, 1960; Greene-Kelley, 1962; Keren and Shainberg, 1975, 1979; and others). Alternatively, smectites in states of partial hydration can be regarded as solid solutions of hydrous and anhydrous smectite components. This formalism facilitates thermodynamic analysis of experimental data and permits correlation of the thermodynamic consequences of smectite dehydration with the interstratification of hydrous and anhydrous layers similar to those responsible for X-ray diffractograms of mixed-layered clays. Accordingly, partially hydrated smectite is regarded in the present communication as a solid solution of hydrous and anhydrous smectite components, described below in terms of regular solution theory.

SOLID SOLUTION MODEL OF SMECTITE DEHYDRATION

Although the 2:1 silicate layers and exchange sites in smectite accommodate many different cations (Schultz, 1969; Weaver and Pollard, 1973; Newman and Brown, 1987), the dehydration of a generic smectite crystallite can be described in terms of an intracrystalline reversible reaction between a symbolic hydrous component (*hs*) and its homologous anhydrous counterpart (*as*) by writing

$$hs \rightleftarrows as + n_c H_2O \tag{2}$$

where n_c stands for the stoichiometric number of moles of interlayer H_2O in one mole of the hydrous component. The law of mass action for reaction (2) can be written as

$$K = \frac{a_{as} a_{H_2O}^{n_c}}{a_{hs}} \tag{3}$$

where K represents the equilibrium constant for reaction (2), a_{H_2O} stands for the activity of H_2O in the aqueous phase, and a_{hs} and a_{as} denote the activities of the hydrous and anhydrous smectite components of the solid

---

[2] For example, the number of moles of interlayer H_2O (n_{il}) in one mole of a given smectite can be described in terms of the mole fraction of the $NaAl_3Si_3O_{10}(OH)_2 \cdot 4.5\ H_2O$ component given in table 1 by first dividing n_{il} by 4.5, which yields $X_{NaAl_3Si_3O_{10}(OH)_2 \cdot 4.5\ H_2O}$ in the smectite (Ransom and Helgeson, 1993).

solution, respectively.[3] The activities of these hydrous and anhydrous smectite components can be expressed in terms of the mole fractions (X_{hs} and X_{as}, respectively) and activity coefficients (λ_{hs} and λ_{as}) of the components by taking account of

$$a_{hs} = X_{hs}\lambda_{hs} \tag{4}$$

and

$$a_{as} = X_{as}\lambda_{as} \tag{5}$$

Substituting eqs (4) and (5) into eq (3) leads to

$$K = \frac{X_{as}\lambda_{as}a_{H_2O}^{n_c}}{X_{hs}\lambda_{hs}}. \tag{6}$$

For a binary system,[4] the logarithmic analog of eq (6) can be combined with

$$X_{as} = 1 - X_{hs} \tag{7}$$

to give

$$\log K = \log\left(\frac{1 - X_{hs}}{X_{hs}}\right) + \log\left(\frac{\lambda_{as}}{\lambda_{hs}}\right) + n_c \log a_{H_2O}. \tag{8}$$

Consideration of experimental data indicates that solid solutions of homologous hydrous and anhydrous smectite components at 25°C and 1 bar are not ideal (see app. A). In contrast, these data are consistent with regular solution theory, which requires random mixing of the hydrous and anhydrous components.

Regular solution theory.—The excess molal Gibbs free energy of mixing (G_{xs}) for binary solid solutions[4] of homologous hydrous and anhydrous smectite components can be expressed in terms of regular solution theory by writing

$$G_{xs} = W_s X_{as} X_{hs} \tag{9}$$

which is consistent with

$$\log \lambda_{as} = \frac{W_s}{2.303\ RT}(1 - X_{as})^2 \tag{10}$$

and

$$\log \lambda_{hs} = \frac{W_s}{2.303\ RT}(1 - X_{hs})^2 \tag{11}$$

[3] The standard state for minerals and water adopted in the present study is one of unit activity of the pure solid or liquid at any pressure and temperature. The standard state for gases calls for unity fugacity of the hypothetical ideal gas at 1 bar and any temperature.

[4] The terms "binary system" and "binary solid solution" refer in the present context to any aluminous dioctahedral smectite solid solution consisting of a single hydrous component and its anhydrous counterpart or a single hydrous endmember and its corresponding anhydrous endmember, both of which are composed of thermodynamic components with specified mole fractions. Hence, the terms apply to strictly binary systems as well as pseudobinary subsystems of multicomponent solid solutions.

where R stands for the gas constant, T represents temperature in Kelvins, and W_s denotes the Margules parameter for the solid solution, which is independent of pressure and temperature. Taking account of eq (8), a function Φ can be defined as

$$\Phi \equiv \log\left(\frac{1 - X_{hs}}{X_{hs}}\right) + n_c \log a_{H_2O}. \tag{12}$$

Combining this expression with eqs (7), (8), (10), and (11) leads to

$$\Phi = \frac{-W_s}{2.303\ RT}(2X_{hs} - 1) + \log K. \tag{13}$$

It follows from eq (12) that values of Φ can be computed from measured values of X_{hs} as a function of a_{H_2O}, if the stoichiometric number of moles of interlayer H_2O in one mole of the hydrous component (n_c) is known. The computed values of Φ can then be plotted in accordance with eq (13) as a linear function of $2X_{hs} - 1$ with a slope of $-W_s/2.303\ RT$ and an intercept of log K.

Stoichiometric number of moles of interlayer H_2O in hydrous smectite components.—Heat of immersion measurements of Na- and Ca-smectite (Keren and Shainberg, 1975; and others) indicate that only interlayer H_2O molecules associated with smectite basal spacings of $\sim 15.7\text{Å}$ or less have thermal properties significantly different from those of bulk water. This observation is supported by compaction studies of argillaceous sediments by van Olphen (1965) and Rieke and Chilingarian (1974), together with X-ray diffraction (XRD) analysis and density measurements of Gulf Coast shales (Powers, 1967; Burst, 1969; Perry and Hower, 1972; Bruce, 1984) which suggest that in the subsurface, dioctahedral aluminous smectites have basal spacings that range from ~ 10 to 15.7 Å. The first of these two spacings correspond to smectite with no interlayer H_2O, and the second to those with hydrated interlayers. Although smectite samples immersed in water or exposed to activities of H_2O close to unity may exhibit basal spacings larger than 15.7 Å in the laboratory, this is probably not the case in nature because geostatic pressures generated during compaction are apparently sufficient to expell interlayer H_2O in excess of that consistent with a 15.7 Å basal spacing. In contrast, pressures far exceeding those along normal geotherms are required to expel interlayer H_2O from smectites with basal spacings ≤ 15.7 Å (van Olphen, 1963). It thus appears that only the number of H_2O molecules required to saturate a smectite interlayer with a ~ 5.7 Å basal spacing (which is equal to twice the effective diameter of the H_2O dipole; Rao, 1972) can contribute to the thermodynamic properties of the mineral. Consideration of the molal volume of the ~ 5.7 Å interlayer and the density of interlayer H_2O indicates that this number is 4.5 moles of H_2O per $O_{10}(OH)_2$ (see below).

The number of interlayer H_2O molecules required to increase the 10 Å basal spacing of an anhydrous smectite to 15.7 Å can be estimated from the unit cell parameters of smectite and the density of interlayer H_2O. The increase in the molal volume of the interlayer caused by this hydration can then be approximated from the 5.7 Å thickness of the

interlayer, provided that the a, b, and β unit cell parameters of the smectite (which is monoclinic) are known. The relation of these parameters to the molal volume of the interlayer (V_{il}) is given by

$$V_{il} = \left(\frac{abc \cos (90 - \beta)}{10^{24} Z}\right) N_0 \qquad (14)$$

where a, b, and β refer to unit cell parameters of smectite, c designates the 5.7 Å thickness of the interlayer, Z denotes the number of chemical formula units in the unit cell, and N_0 stands for Avogadro's number.

Owing to the small size of smectite crystallites and their intimate association with other structurally similar minerals in clay samples, most XRD data for this mineral are not sufficiently comprehensive or accurate to permit retrieval of reliable unit cell parameters. However, unit cell parameters for chemically and structurally similar dioctahedral 2:1 phyllosilicates such as muscovite, pyrophyllite, and paragonite are well known. Taking account of the similarity in the crystal structure and the composition of the octahedral and tetrahedral layers of dioctahedral aluminous smectite and pyrophyllite, the a, b, and β unit cell parameters of pyrophyllite were used in the present study to approximate the lateral dimensions of a typical smectite 2:1 silicate layer. Taking $c = 5.7$ Å in eq (14) as the thickness of the hydrated interlayer and adopting the values of $a = 5.172$ Å, $b = 8.958$ Å, $\beta = 100°$, and $Z = 2$ for pyrophyllite reported by Bailey (1980) leads to $V_{il} = 78.3$ cm³/mol. The volume of the interlayer cation in smectite can be approximated by that of Na^+, which has a molal volume of ~ 2.66 cm³. Subtracting 0.3 of this value from 78.3 cm³/mol results in 77.5 cm³/mol for the volume occupied by the interlayer H_2O dipoles in one mole of smectite containing $O_{10}(OH)_2$ and 0.3 moles of interlayer Na^+.

Experimental studies at elevated temperatures and pressures suggest that the volume of reaction (2) is positive, which requires the density of H_2O in smectite interlayers to be greater than that of bulk H_2O (Khitarov and Pugin, 1966; Koster van Groos and Guggenheim, 1984, 1986, 1987; Colten, 1986; Hall, Astill, and McConnell, 1986). These observations are supported by neutron diffraction measurements at 25°C and 1 bar by Hawkins and Egelstaff (1980), who report the density of interlayer H_2O to be ~ 1.05 g/cm³ in Na-smectite with a basal spacing of ~ 15.7 Å.[5] In the absence of excess H_2O,[6] most hydrated smectites exhibit

---

[5] Values of what is referred to in the literature as the density of interlayer H_2O range from 0.85 to 1.43 g/cm³ (Martin, 1962). However, in most cases these values are derived from bulk densities. Consequently, many of the reported densities do not correspond to grams of interlayer H_2O per cubic centimeter of interlayer H_2O but instead represent total grams of H_2O per cubic centimeter of interlayer volume. This is not true of the density of interlayer H_2O reported by Hawkins and Egelstaff (1980), which was obtained from neutron diffraction measurements.

[6] Excess H_2O is defined in the present study as any H_2O in excess of 4.5 moles per $O_{10}(OH)_2$. Excess H_2O commonly occurs in turbostratic layer silicates at activities of $H_2O >$ 0.9. Under these circumstances, each 2:1 silicate layer has its own coulombic potential. Consequently, these layers adsorb H_2O independently of the other layers in the sample, resulting in vertical separation of individual clay layers from one another by many tens of angstroms.

the same ~ 5.7 Å interlayer spacing, regardless of the composition of the 2:1 silicate layer or the number and type of cations in the interlayer (Glaser and Mering, 1968; Roderick, Senich, and Demirel, 1969; Suquet, de la Calle, and Pezerat, 1975; Omerod and Newman, 1983; and others). Hence, both V_{il} computed from eq (14) and the density of interlayer H_2O reported by Hawkins and Egelstaff (1980) were taken in the present study to be independent of the smectite 2:1 silicate layer composition and the number and identities of the cations on the exchange sites. This density (1.05 g/cm³) was combined with the interlayer volume computed from eq (14) to evaluate n_c (the number of moles of H_2O in a hypothetical fully hydrated smectite interlayer) from

$$n_c = \frac{\rho_{il}V_{il}}{M_w} = \frac{(1.05)(77.5)}{18.0153} = 4.5 \tag{15}$$

where ρ_{il} stands for the density of interlayer H_2O, and M_w denotes the molecular weight of water. It follows from eq (15) that a hypothetical fully hydrated smectite interlayer with a typical interlayer site occupancy of 0.3 cations per $O_{10}(OH)_2$ contains 15 H_2O dipoles per mole of monovalent cation (see below). This number of H_2O dipoles is in close agreement with estimates of the number of interlayer H_2O dipoles in smectite (12-16 per mole of monovalent cation) that have been reported in the literature (Keren and Shainberg, 1975; Omerod and Newman, 1983).

It has been argued that the composition of the 2:1 layers in aluminous dioctahedral smectite and the location and magnitude of tetrahedral and octahedral layer charges have an appreciable effect on the amount of interlayer H_2O in the mineral (Tardy and Touret, 1987; Newman and Brown, 1987; Tardy and Duplay, 1992). However, these arguments fail to distinguish explicitly between interlayer H_2O and that in pores and adsorbed on the exposed surfaces of the particles in the clay sample. Furthermore, the arguments are not based on simultaneous consideration of both hydration and dehydration isotherms, which is a necessary requirement to bracket unambiguously the equilibrium composition of the clay. Studies by Foster (1953, 1955), Davidtz and Lowe (1970), and Eberl, Srodon, and Northrop (1986) of tetrahedral occupancy in aluminous dioctahedral smectites as a function of their total hydration state reveal no consistent correlation between tetrahedral charge and the total H_2O taken up by the minerals. In addition, both theory and experiment indicate that changes in the b-dimension are primarily responsible for swelling of smectite samples, rather than isomorphous substitution accompanied by a change in the octahedral layer charge (Davidtz and Lowe, 1970). As noted by Newton (1987), the amount of H_2O adsorbed in pores and on the surfaces of 2:1 layer silicate particles that do not contain interlayer H_2O (for example, muscovite, illite, et cetera) is proportional to surface area and surface charge. This is

also true for the adsorption of H_2O on the external surfaces of smectite particles (Newton, 1987). Because interlayer charge is satisfied by cations and the number of those in the interlayer are constrained by layer lattice charges and dimensions, smectites adsorb H_2O primarily on external particle surfaces at high partial pressures of H_2O.

The distribution of cations and H_2O dipoles in a hydrated smectite interlayer is shown schematically in figure 1, where it can be seen that each monovalent cation is associated with 15 molecules of H_2O. The distribution of interlayer H_2O dipoles shown in this figure is similar to that proposed by Mathieson and Walker (1954) for vermiculite. The shaded triangular areas in the figure represent the faces of silica tetrahedra at the base of the interlayer. The white circles designate H_2O dipoles above the plane of the interlayer, and the hatched circles indicate those below. Monovalent interlayer cations are represented by the black circles, which are distributed in an ordered arrangement on the interlayer sites in order to minimize intermolecular electrostatic repulsion. Vacant interlayer sites are designated in figure 1 by the letter V.
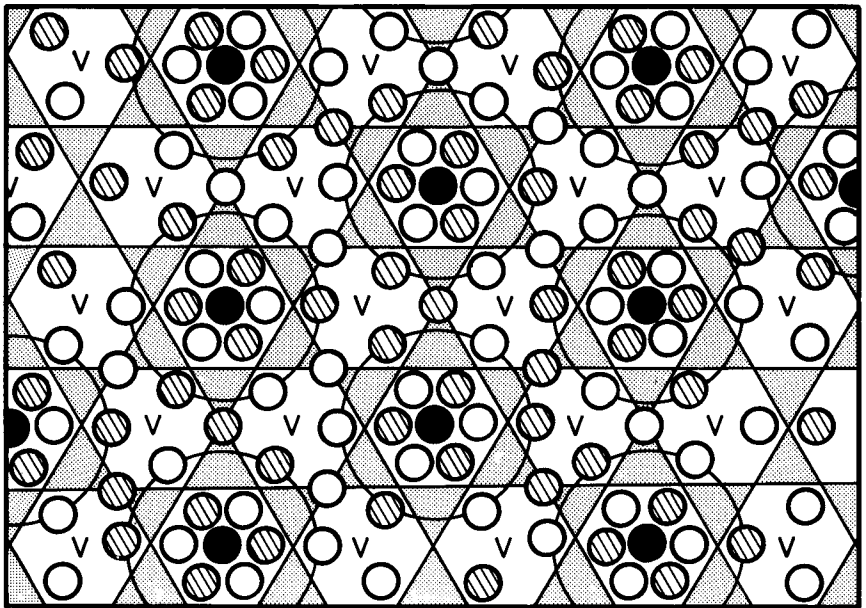
Fig. 1. Schematic plan view of an idealized smectite interlayer containing 15 molecules of interlayer H_2O per monovalent cation. Monovalent interlayer cations and vacant interlayer sites are designated by black circles and the letter V, respectively. H_2O dipoles in primary, secondary, and tertiary coordination around the cations are represented by white and hatched circles denoting H_2O dipoles above and below the plane of the interlayer sites, respectively. The H_2O dipoles in the secondary hydration shells are linked by arcs. The shaded triangular areas represent the faces of the silica tetrahedra in the underlying tetrahedral sheet.

Although the number of moles of H_2O dipoles in the interlayer depicted in figure 1 is independent of the 2:1 silicate layer composition, the distribution of the dipoles within the interlayer depends on the identity of the interlayer cation. Six H_2O dipoles are depicted schematically in primary octahedral coordination around each of the exchange cations shown in this figure. More loosely held secondary hydration shells coincide with the H_2O dipoles connected by the arcs in figure 1. The H_2O dipoles that fall outside the secondary shells can be considered to be in tertiary coordination around the cation. The latter H_2O dipoles are more loosely held than those in either primary or secondary coordination and are shared between adjacent hydrated cations. According to the model proposed in the present communication, continuous exchange occurs among the vacancies and H_2O dipoles in the various hydration shells so that homogeneous equilibrium is maintained throughout the interlayer. The structural model shown in figure 1 is consistent with the observation that interlayer H_2O has a liquid-like structure that is not highly ordered into definite planes of molecules in rigid association with the smectite 2:1 silicate layer (Hawkins and Egelstaff, 1980; Hall, 1981; Sposito and Prost, 1982).

The distribution of H_2O dipoles shown in figure 1 pertains only to smectites with interlayers in which 30 percent of the interlayer sites are occupied by monovalent cations. For smectites with different monovalent exchange cation occupancies or those with divalent interlayer cations, the distribution of H_2O dipoles should be similar in geometry but different in detail, depending on the number and valence of the interlayer cations and the degree of positional disorder between these cations and the interlayer sites. For example, interlayer Na^+ should have a greater number of H_2O dipoles in primary coordination than K^+, which has a lower hydration number in aqueous solution. Note that the net positive charge associated with the interlayer cations is neutralized by the net negative charge on the over- and underlying 2:1 silicate layers. Therefore, any increase or decrease in the number or valence of the cations in the interlayer sites causes rearrangement, but no change in the number of H_2O dipoles present in the interlayer.

REGRESSION ANALYSIS OF EXPERIMENTAL DATA

Smectite water-vapor pressure isotherm studies involve measurement of the uptake and release of H_2O vapor by smectite samples in response to changes in relative humidity (Barshad, 1955, 1960; Mooney, Keenan, and Wood, 1952; Greene-Kelley, 1962; Martin, 1962; Fripiat and others, 1965; Roderick, Senich, and Demirel, 1969; Keren and Shainberg, 1975, 1979, 1980; Omerod and Newman, 1983; Tardy and Touret, 1987; Kraehenbuehl and others, 1987; Tardy and Duplay, 1992; and others). These experiments leave unchanged the identities of the interlayer cations and the composition of the 2:1 silicate layers in the smectite sample. Although the hydration and dehydration isotherms for a given sample do not generally coincide with one another, each isotherm bounding the hysteresis represents a continuum of H_2O concentrations

ranging from zero to many hundreds of milligrams of H_2O per gram of dry clay.

The hysteresis between the hydration and dehydration isotherms of smectite samples has been the subject of considerable discussion. It is generally attributed to effects such as changes in surface area, pore structure, sample history, and the structure of adsorbed H_2O with increasing or decreasing activity of H_2O, as well as kinetic inhibitions, rates of diffusion, and capillary condensation and restriction (Bangham, 1944; Mooney, Kennan, and Wood, 1952; Barshad, 1955, 1960; Johansen and Dunning, 1959; Martin, 1959; van Olphen, 1965; Fripiat and others, 1965; Gregg and Sing, 1967; Roderick, Senich, and Demirel, 1969; Keren and Shainberg, 1975; Lecloux and Pirard, 1979; Mason, 1982; Bransom and Newman, 1983; Omerod and Newman, 1983; Delon and others, 1986; Kraehenbuehl and others, 1987; Newman, 1987; and others). Although neither the hydration nor dehydration isotherm necessarily represents equilibrium between smectite and the vapor phase, many attempts have nevertheless been made to determine standard state thermodynamic properties of smectite and interlayer H_2O directly from smectite-water vapor-pressure isotherms. In some cases, hydration isotherms have been used for this purpose (van Olphen, 1965; Roderick, Senich, and Demirel, 1969; Keren and Shainberg, 1975, 1979, 1980; Hall and Astill, 1989). In others, dehydration isotherms were used (Mooney, Keenan, and Wood, 1952; Bird, 1984; Tardy and Touret, 1987; Tardy and Duplay, 1992). In still others, each isotherm was used independently to derive a value for a given thermodynamic property, thereby generating more than one value of the same property at the same partial pressure of H_2O (Barshad, 1960; Tardy and others, 1980), *which violates the requirement that the derivatives of these properties be exact differentials.* Despite the fact that neither the hydration nor dehydration isotherm necessarily represents the equilibrium state of the system, the two isotherms taken together can be considered to bracket the equilibrium values of X_{hs} and the activity of H_2O (see below).

Smectite water-vapor pressure isotherms represent the total concentration of H_2O taken up by the sample, which is distributed among the interlayers, the outer surfaces of particles, and the open pore spaces in the sample. In order to retrieve standard state thermodynamic properties for smectite dehydration from such data, the amount of H_2O in excess of that in the interlayer must be assessed and subtracted from the total amount taken up by the clay sample. The remaining amounts of H_2O consistent with the hydration and dehydration isotherms can then be used to calculate values of X_{hs} that bracket the equilibrium concentration of interlayer H_2O in the clay sample in a manner analogous to reversal brackets in phase equilibrium studies such as those analyzed by Helgeson and others (1978), Berman and Brown (1985), Newton (1987), and others. Paired hydration and dehydration isotherm data which constitute the limits of these brackets can then be regressed to assess standard state thermodynamic properties for the dehydration process (see below).

Despite arguments to the contrary (Tardy and Touret, 1987; Tardy and Duplay, 1992), only internally consistent studies in which both hydration and dehydration isotherms have been determined for smectite samples that have been physically and chemically well characterized can be used with confidence to retrieve equilibrium standard state thermodynamic properties for the hydration of smectite. Both of these isotherms must be used to bracket the equilibrium hydration state of the smectite. The smectite isotherm data at 25°C and 1 bar reported by Keren and Shainberg (1975) for the Wyoming Montmorillonite (API No. 25) can be used for this purpose. Accordingly, these data were used in the present study to retrieve Margules parameters and equilibrium constants representing homogeneous equilibrium between the hydrous and anhydrous components of Na- and Ca-smectites. The results of these calculations were subsequently used to estimate equilibrium constants and Margules parameters for other smectite solid solutions.

Calculation of X_{hs} from water vapor-pressure isotherm data for Na- and Ca-smectites.—The relative distribution of H_2O among the interlayers and that in pores and adsorbed on particle surfaces in the smectite samples studied by Keren and Shainberg (1975) can be approximated by comparing their isotherms with those for a similar mineral that does not adsorb interlayer H_2O. Kaolinite was chosen for this purpose because the H_2O adsorbed by kaolinite samples occurs only in pores and on particle surfaces, and kaolinite is the closest structural analog to smectite for which pure samples are available. Nitrogen adsorption measurements for kaolinite and smectite reported by Johansen and Dunning (1959) indicate that the external surface area of the kaolinite they studied was approximately one half that of Na-saturated Clay Spur Montmorillonite, API No. H-26, which is similar in composition to that used by Keren and Shainberg (1975). Johansen and Dunning (1959) report surface areas of 16 m^2/g and 38 m^2/g for their kaolinite and smectite samples, respectively. These values compare favorably with other external surface area measurements of 18.6·m^2/g reported by Mooney, Keenan, and Wood (1952) for kaolinite and 27 m^2/g given by Kennan, Mooney, and Wood (1951) for smectite. Although nitrogen adsorption data were not reported for the smectite samples used by Keren and Shainberg (1975), their hydration/dehydration isotherms for Na-saturated Wyoming Montmorillonite are consistent with those reported by Johansen and Dunning (1959) for the Na-saturated Clay Spur Montmorillonite (see below). This observation suggests that the amount of H_2O taken up in pores and on the external surfaces of the smectite particles in the two studies are comparable. Hence, the amount of H_2O adsorbed on the particles in one gram of the smectite studied by Keren and Shainberg (1975) was taken to be approximately twice that adsorbed on the particle surfaces of 1 g of the kaolinite sample reported by Johansen and Dunning (1959).

To calculate the amount of interlayer H_2O present in the smectite samples analyzed by Keren and Shainberg (1975), twice the number of grams of H_2O adsorbed per gram of dry kaolinite reported by Johansen and Dunning (1959) was subtracted from the number of grams of H_2O

adsorbed per gram of dry smectite reported for the same activity of H_2O by Keren and Shainberg (1975). Because the Na- and Ca-saturated smectites used by Keren and Shainberg (1975) were derived from splits of a single sample, the amount of H_2O adsorbed on the external surfaces and pores was taken in the present study to be the same for each of the clay samples. The concentration of interlayer H_2O in the Na- and Ca-smectite samples studied by Keren and Shainberg (1975) was then calculated and recast into moles of interlayer H_2O per mole of clay (n_{il}) with the aid of

$$n_{il} = \frac{(g_s - 2g_k)M_s}{M_w} \qquad (16)$$

where g_s and g_k represent the total number of grams of H_2O taken up by smectite (Keren and Shainberg, 1975) and kaolinite (Johansen and Dunning, 1959), respectively, and M_w and M_s stand for the molecular weight of water and smectite. The results of these calculations were then used to compute the concentrations of interlayer H_2O in the smectite samples, which can be expressed as the mole fraction of the hydrated smectite component (X_{hs}) of the solid solution by taking account of

$$X_{hs} = \frac{n_{il}}{4.5} \qquad (17)$$

where 4.5 corresponds to the value of n_c calculated from eq (15).

Regression analysis of isotherm data for Na- and Ca-smectite.—Circles representing isotherm data reported by Keren and Shainberg (1975) for Wyoming Montmorillonite are plotted in figures 2 and 3, where relative humidities are plotted against corresponding values of X_{hs} computed from eq (17). Hydration and dehydration data are designated in these figures by white and black symbols, respectively. Pairs of hydration and dehydration data at either the same relative humidity or the same approximate H_2O concentration in smectite are denoted by symbols that are half black and half white or are connected by short straight lines. These symbols bracket the equilibrium hydration state of the smectite. Using the procedure outlined above, values of X_{hs} in smectite were also computed for the compositionally-similar Na-saturated Clay Spur Montmorillonite from the isotherm and nitrogen adsorption data reported by Johansen and Dunning (1959). These data are represented by the triangles in figure 2, where they can be compared with those retrieved from data for Wyoming Montmorillonite reported by Keren and Shainberg (1975). It can be seen in this figure that the mole fractions of interlayer H_2O taken up by the two Na-smectites are in close agreement at relative humidities ≤ 0.8, where the effects of differences in the surface areas of the two samples on X_{hs} should be small. Note that the data generated from both studies bracket the same approximate values of X_{hs} and relative humidity, despite the fact that they represent different smectite samples studied by different investigators. Adopting the assump-
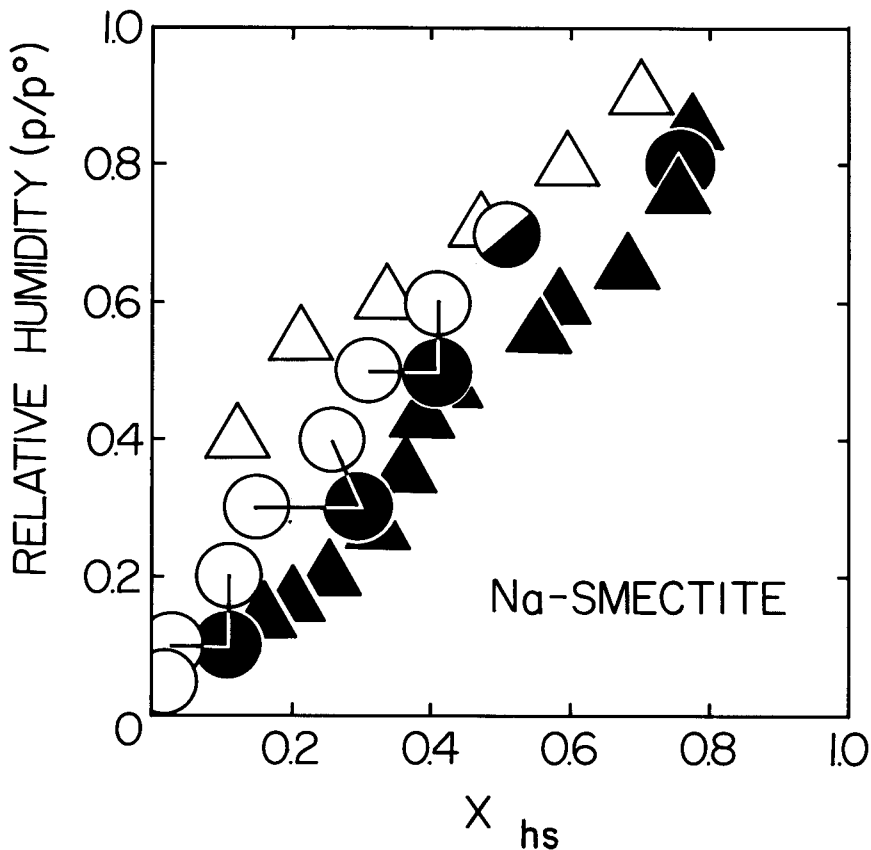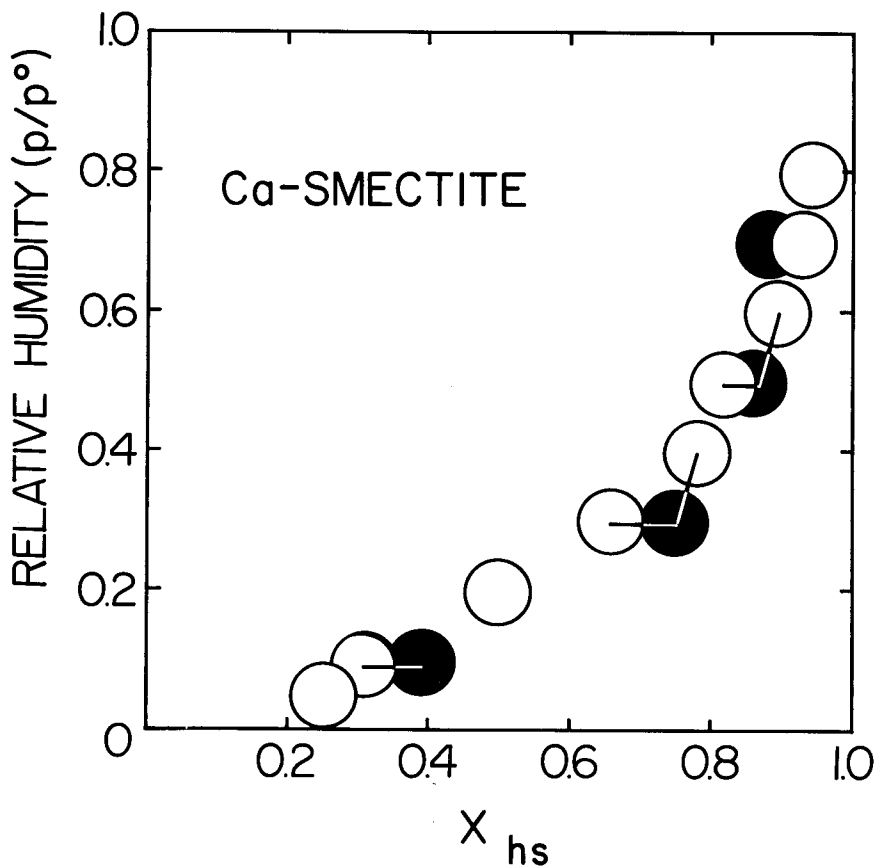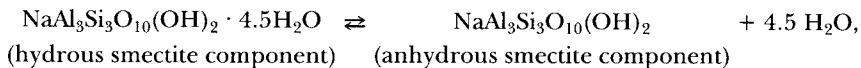
Fig. 2. Relative humidity as a function of the mole fraction of the hydrated component (X_{hs}) of a Na-smectite solid solution of hydrous and anhydrous components at 25°C and 1 bar. The white and black symbols represent hydration and dehydration isotherm data, respectively. The circles denote Na-smectite water-vapor pressure data reported by Keren and Shainberg (1975), and the triangles represent vapor pressure data taken from Johansen and Dunning (1959), which were adjusted in the present study with the aid of eqs (16) and (17) to eliminate the effect of H_2O adsorbed in pores and on particle surfaces. The half black and half white symbol and those connected by short straight lines bracket the equilibrium composition of the smectite (see text).

tion that the hydration and dehydration of smectite is independent of the 2:1 silicate layer composition (see above), the experimental data represented by the circles in figures 2 and 3 can be used to determine the equilibrium hydration state of dioctahedral aluminous Na- and Ca-smectites.

Paired sets of hydration and dehydration isotherm data taken from Keren and Shainberg (1975) were used to bracket equilibrium smectite hydration states and general values of $\log K$ and W_s from eq (13) by writing reaction (2) in terms of binary solid solutions of hydrous and

Fig. 3. Relative humidity as a function of the mole fraction of the hydrous component (X_{hs}) of a Ca-smectite solid solution of hydrous and anhydrous components at 25°C and 1 bar (see caption of fig. 2).

anhydrous smectite components. One such reaction can be expressed as

$$NaAl_3Si_3O_{10}(OH)_2 \cdot 4.5H_2O \quad \rightleftharpoons \quad NaAl_3Si_3O_{10}(OH)_2 \quad + 4.5\ H_2O,$$
(hydrous smectite component)   (anhydrous smectite component)

(18)

where $NaAl_3Si_3O_{10}(OH)_2 \cdot 4.5\ H_2O$ and $NaAl_3Si_3O_{10}(OH)_2$ represent two of the thermodynamic components of smectite solid solutions shown in table 1. The relative humidities plotted in figures 2 and 3 are equivalent to activities of H_2O (a_{H_2O}) referenced to the liquid standard state (see app. B). Hence, the values of relative humidity reported for the isotherm data shown in these figures can be substituted directly for a_{H_2O} in eq (12). Because the dehydration process does not change the identity of the
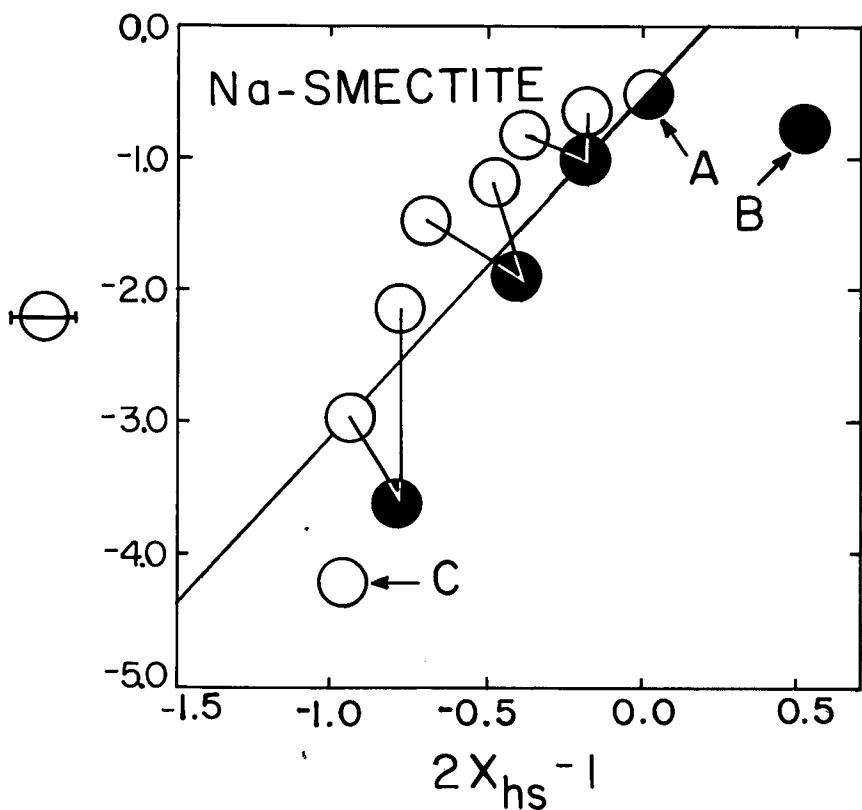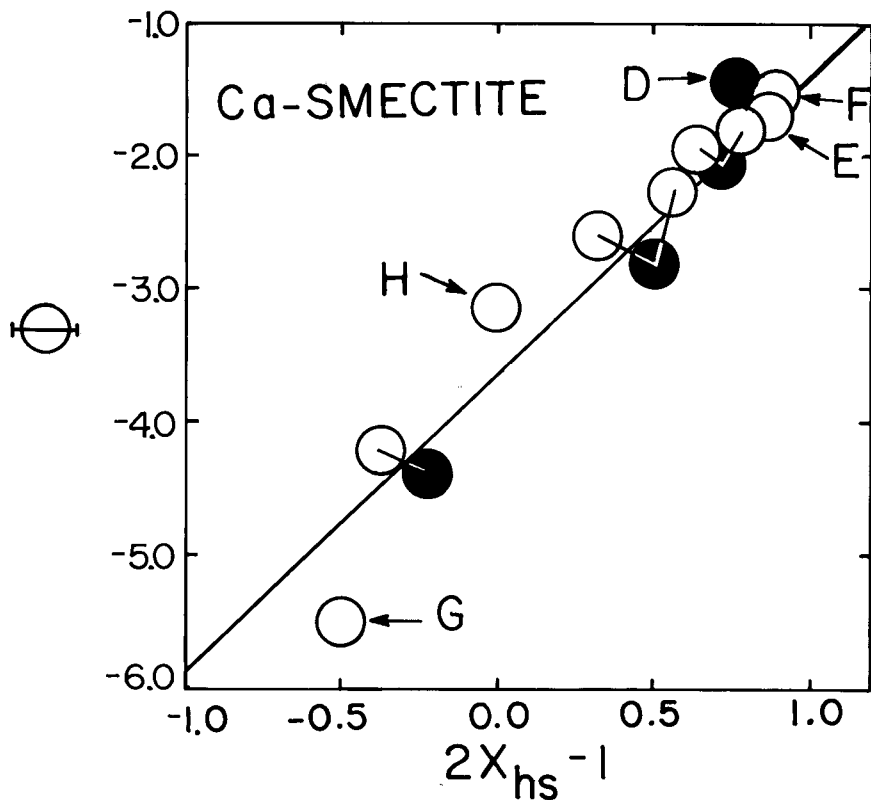
Fig. 4. Values of Φ computed from eq (12) as a function of $2X_{hs} - 1$ for the Na-smectite isotherms shown in figure 2. The symbols and reaction brackets correspond to those described in the caption of figure 2. The straight line drawn through the symbols was generated by graphical regression of the data. Data points A, B, and C are discussed in the text.

interlayer cation or the composition of the silicate layers in the sample, the values of X_{hs} shown in figures 2 and 3 and the corresponding values of a_{H_2O} permit calculation of Φ from eq (12). These values can then be regressed with eq (13) as a function of $2X_{hs} - 1$ to generate values of W_s and log K for Na- and Ca-smectite dehydration at 25°C and 1 bar. Regression calculations of this kind resulted in the straight lines drawn through the brackets shown in figures 4 and 5. The symbols and brackets in these figures are the same as those shown in figures 2 and 3. The experimental data used in the regression calculations include those that terminate the isotherm brackets in figures 4 and 5, as well as the data represented by the symbols labeled A, B, E, F, and H. The symbol labeled A represents the intersection of the hydration and dehydration isotherms reported by Keren and Shainberg (1975). Although symbols B, E, F, and H do not define brackets, each is consistent with the equilibrium con-

Fig. 5. Values of Φ computed from eq (12) as a function of $2X_{hs} - 1$ for the Ca-smectite isotherm shown in figure 3. The symbols and reaction brackets correspond to those described in the caption of figure 3. The straight line drawn through the symbols was generated by graphical regression of the data. Data points D, E, F, G, and H are discussed in the text.

traints imposed by the isotherm brackets shown in figures 2 to 5. The symbols labeled C, D, and G in figures 4 and 5 are inconsistent with these constraints. Accordingly, the data represented by these symbols were excluded from the regression calculations. In the case of the data represented by symbols C and G, large uncertainties attend calculation of n_{il} from eq (16), because only small amounts of H_2O are taken up by the samples at relative humidities < 0.1. The data represented by symbol D are inconsistent with the reaction brackets determined by the other data for Ca-smectite.

The regression lines shown in figures 4 and 5 were generated by first assessing maximum and minimum allowable slopes and intercepts for straight lines drawn through the brackets of the Na- and Ca-smectite isotherm data. The averages of the maximum and minimum slopes and intercepts, respectively, were then used to construct the lines shown in

the figures, from which values of log K and W_s for Na- and Ca-smectite were computed with the aid of eq (13). These values are given in table 3. The uncertainties in the values of log K for Na- and Ca-smectite are ±0.004 and ±0.19, respectively, and those associated with the corresponding values of W_s are ±34 cal/mol and ±388 cal/mol. These uncertainties represent the maximum and minimum values of log K and W_s required to fit the reaction brackets shown in figures 4 and 5. The values of log K and W_s for Na- and Ca-smectite shown in table 3 were used together with eqs (12) and (13) to generate the curves shown in figures 6 and 7.

The solid curves shown in figures 6 and 7 correspond to the calculated equilibrium hydration state of Na- and Ca-smectite for regular
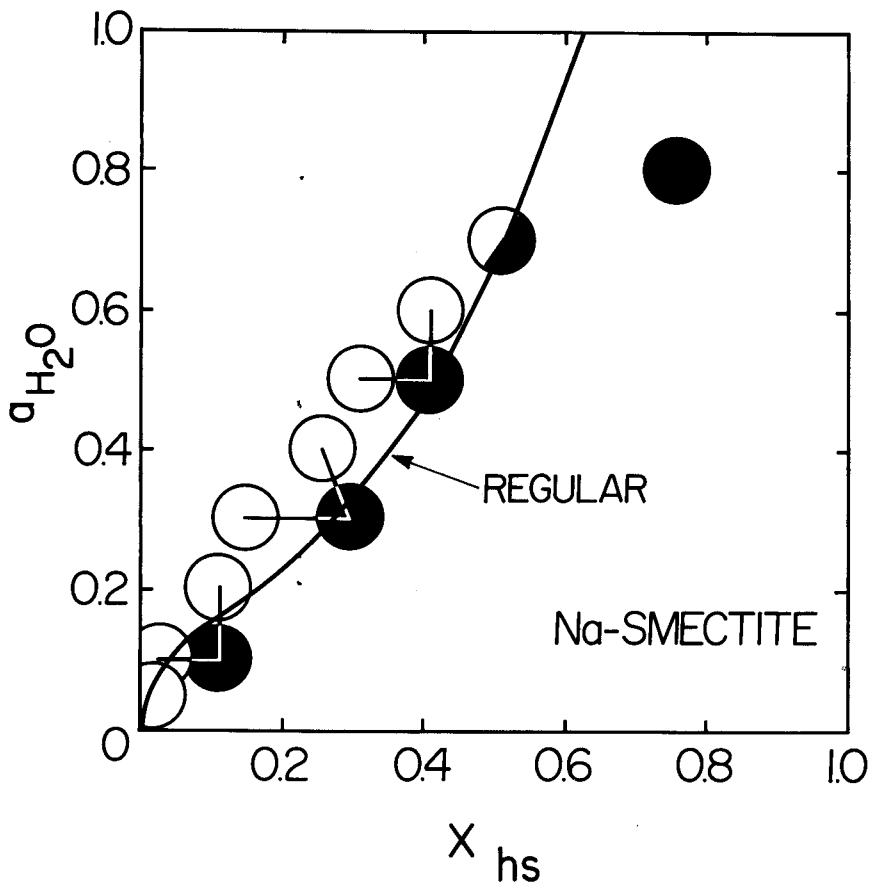
Fig. 6. Activity of H_2O as a function of the mole fraction of the hydrous component (X_{hs}) of Na-smectite assuming a regular solid solution of hydrous and anhydrous smectite components at 25°C and 1 bar. The curve was generated from eqs (12) and (13) using the Margules parameter (W_s) and equilibrium constant (K) for Na-smectite shown in table 3. The symbols and reaction brackets are the same as those described in the caption of figure 2.
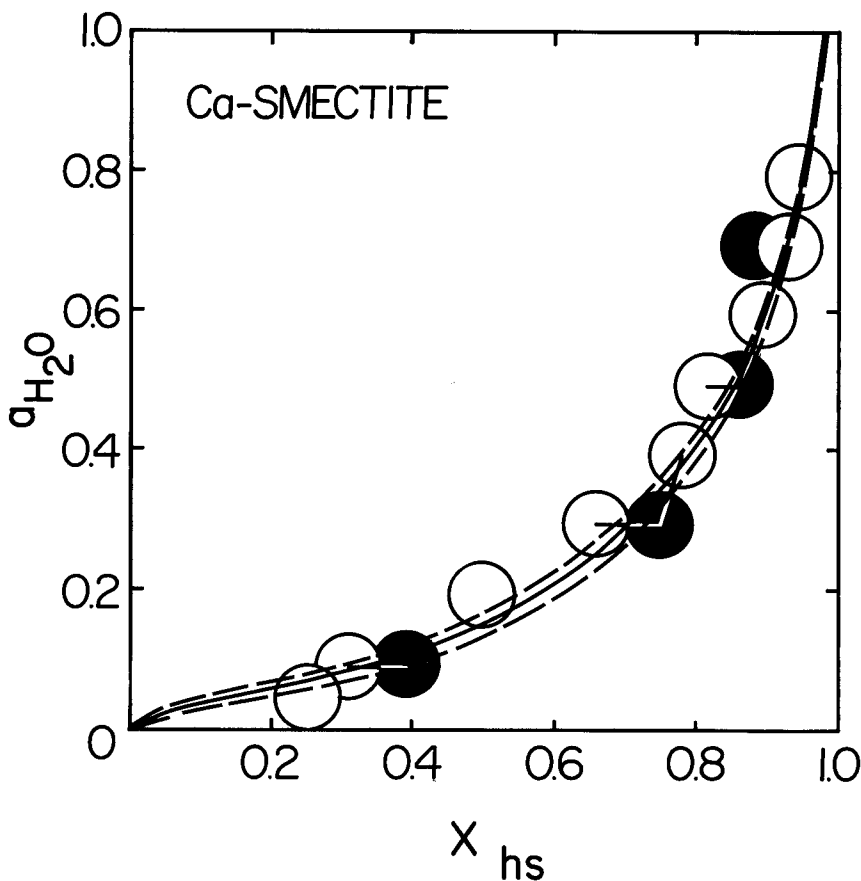
Fig. 7. Activity of H_2O as a function of the mole fraction of the hydrous component (X_{hs}) of Ca-smectite assuming a regular solid solution of hydrous and anhydrous smectite components at 25°C and 1 bar. The curve was generated from eqs (12) and (13) using the Margules parameter (W_s) and equilibrium constant (K) for Ca-smectite shown in table 3. The dashed curves represent maximum and minimum deviations arising from uncertainties in W_s and K. The symbols and reaction brackets are the same as those described in the caption of figure 3.

solid solutions of homologous hydrous and anhydrous smectite components. The uncertainties in the calculations for Ca-smectite are indicated by the dashed curves in figure 7. Corresponding uncertainties are not shown in figure 6, because they fall within the thickness of the curve representing the equilibrium hydration state of Na-smectite. Note in figure 7 that at $a_{H_2O} = 1$, the value of X_{hs} at 25°C and 1 bar is equal to 0.98. Hence, pure Ca-smectite crystals in homogeneous equilibrium are essentially fully hydrated in the presence of water at the Earth's surface. In contrast, the value of X_{hs} for Na-smectite at $a_{H_2O} = 1$ is 0.62 at Earth

surface conditions, and therefore *pure Na-smectite crystals in homogeneous equilibrium are not fully hydrated in natural environments.*

ESTIMATION OF LOG K AND W_S FOR THE DEHYDRATION OF HOMOIONIC HOMOLOGS OF NA- AND CA-SMECTITE

The interlayer sites of most natural smectites are occupied predominantly by Na^+, Ca^{2+}, K^+, and Mg^{2+}. However, NH_4^+, Rb^+, Cs^+, Ba^{2+}, and Sr^{2+} commonly occur as interlayer cations in smectites found in petroliferous shales and nuclear waste repository sites. Of the smectites containing one or more of these various cations, insufficient experimental data are available to permit direct retrieval of equilibrium constants and Margules parameters for all but the Ca- and Na-smectites. In the absence of such data, the standard molal Gibbs free energies of dehydration for smectite solid solutions can be estimated if the 2:1 silicate layers contribute negligibly to the standard molal Gibbs free energy of reaction (2), which seems to be the case. Under these conditions, ΔG_r° for reaction (2) correspond to $-\Delta G_r^\circ$ for the reaction representing solvation of the interlayer cation, which is analogous to that of cations in water.

It has been shown (Helgeson, Kirkham, and Flowers, 1981) that the standard partial molal Gibbs free energy of solvation of the jth cation in an aqueous solution (ΔG_j°) can be described in terms of its charge (Z_j) and effective electrostatic radius ($r_{e,j}$) by writing the Born transfer equation (Born, 1920; Bjerrum, 1929) as

$$\Delta G_j^\circ = \omega_j \left(\frac{1}{\epsilon} - 1 \right) \tag{19}$$

where ϵ designates the dielectric constant of H_2O, and ω_j stands for the Born coefficient of the jth cation, which is given by

$$\omega_j = \frac{\eta Z_j^2}{r_{e,j}} \tag{20}$$

where η equals 1.66027×10^5 Å cal/mol. It follows from the law of corresponding states that the standard molal Gibbs free energies of solvation for different cations in the smectite interlayer should vary linearly with the standard molal Gibbs free energies of solvation of the same cations in the aqueous state. Hence, ω_j for a series of cations in the interlayer state should correlate linearly with the respective values of ω_j in the aqueous state at 25°C and 1 bar, which leads to

$$\frac{\log K}{Z_l} = a_1 + a_2 \omega_j \tag{21}$$

where Z_l denotes the absolute value of the charge on the 2:1 silicate layer of the mineral per $O_{10}(OH)_2$, a_1 and a_2 stand for temperature- and pressure-dependent parameters independent of the identities and charges of the interlayer cations, and K refers to the equilibrium constant for the solvation reaction in the interlayer. Adopting the same corresponding

states approach to describe the excess molal Gibbs free energy of solvation of interlayer cations leads to

$$W_s = b_1 + b_2\omega_j \tag{22}$$

where b_1 and b_2 stand for the excess molal Gibbs free energy analogs of a_1 and a_2, respectively.

Values of log K and W_s for Na- and Ca-smectite retrieved from isotherm data reported by Keren and Shainberg (1975) were used together with values of ω_j and $r_{e,j}$ taken from Shock and Helgeson (1988) and a typical value for Z_l of 0.3 to generate values of a_1, a_2, b_1, and b_2 from eqs (21) and (22). The calculations resulted in $a_1 = -10.385$, $a_2 = 1.49 \times 10^{-4}$ mol/cal, $b_1 = -3477.2$ cal/mol, and $b_2 = 2.57 \times 10^{-3}$. These values were then combined with eqs (21) and (22) to compute values of log K and W_s at 25°C and 1 bar for binary homoionic K-, NH_4-, Rb-, Cs-, Mg-, Sr-, and Ba-smectite solid solutions of the thermodynamic components listed in table 2. The results of these calculations are shown in table 3, together with corresponding values of ω_j and $r_{e,j}$ taken from Shock and Helgeson (1988). It can be seen in this table that the values of W_s for smectites with monovalent interlayer cations range from -3254 to -3314

TABLE 2

Hydrous and anhydrous thermodynamic components per $O_{10}(OH)_2$ of homologous homoionic binary smectite solid solutions

Anhydrous	Hydrous
$NaAl_3Si_3O_{10}(OH)_2$	$NaAl_3Si_3O_{10}(OH)_2 \cdot 4.5\,H_2O$
$KAl_3Si_3O_{10}(OH)_2$	$KAl_3Si_3O_{10}(OH)_2 \cdot 4.5\,H_2O$
$NH_4Al_3Si_3O_{10}(OH)_2$	$NH_4Al_3Si_3O_{10}(OH)_2 \cdot 4.5\,H_2O$
$RbAl_3Si_3O_{10}(OH)_2$	$RbAl_3Si_3O_{10}(OH)_2 \cdot 4.5\,H_2O$
$CsAl_3Si_3O_{10}(OH)_2$	$CsAl_3Si_3O_{10}(OH)_2 \cdot 4.5\,H_2O$
$Ca_{0.5}Al_3Si_3O_{10}(OH)_2$	$Ca_{0.5}Al_3Si_3O_{10}(OH)_2 \cdot 4.5\,H_2O$
$Mg_{0.5}Al_3Si_3O_{10}(OH)_2$	$Mg_{0.5}Al_3Si_3O_{10}(OH)_2 \cdot 4.5\,H_2O$
$Sr_{0.5}Al_3Si_3O_{10}(OH)_2$	$Sr_{0.5}Al_3Si_3O_{10}(OH)_2 \cdot 4.5\,H_2O$
$Ba_{0.5}Al_3Si_3O_{10}(OH)_2$	$Ba_{0.5}Al_3Si_3O_{10}(OH)_2 \cdot 4.5\,H_2O$

TABLE 3

Electrostatic parameters for eqs (21) and (22), and Margules parameters (W_S) and values of log K, ΔG°_r, and X_{hs} for the dehydration of various homologous homoionic binary smectite solid solutions represented by reaction (2) at 25°C and 1 bar

Solid Solution	$r_{e,j}$† (Å)	ω_j† (kcal/mol)	W_S* (kcal/mol)	log K**	ΔG°_r (kcal/mol)	X_{hs}††
Na-smectite	1.91	86.925	−3.254§	−0.767§	1.047	0.62
K-smectite	2.27	73.140	−3.289	−0.151	0.207	0.52
NH$_4$-smectite	2.31	71.873	−3.293	−0.095	0.129	0.52
Rb-smectite	2.41	68.891	−3.300	0.038	−0.052	0.49
Cs-smectite	2.61	63.612	−3.314	0.274	−0.374	0.46
Mg-smectite	2.54	261.460	−2.806	−4.28	5.842	0.99
Ca-smectite	2.87	231.397	−2.883§	−3.61§	4.926	0.98
Sr-smectite	3.00	221.369	−2.909	−3.39	4.620	0.96
Ba-smectite	3.22	206.245	−2.948	−3.05	4.160	0.94

* Unless indicated otherwise, these values were computed from eq (22).
** Unless indicated otherwise; these values were computed from eq (21).
§ Generated by regression of experimental data reported by Keren and Shainberg (1975) with eqs (12) and (13).
† Values taken from Shock and Helgeson (1988).
†† Computed for $a_{H_2O} = 1$.

cal/mol, and those for smectites with divalent cations from −2806 to −2948 cal/mol. The uncertainties in these values are estimated to be of the order of 10 percent or less. Values of log K for smectites with monovalent cations vary from −0.767 to 0.274, and those for smectites with divalent interlayer cations range from −4.28 to −3.05 with uncertainties estimated to be ≤ 5 percent.

The values of log K given in table 3 were used together with the expression

$$\Delta G^{\circ}_r = -2.303 \, RT \log K \tag{23}$$

to generate values of the standard molal Gibbs free energies of reaction (ΔG°_r) for reaction (2) at 25°C and 1 bar. The results of these calculations are given in table 3. It can be seen in this table that standard molal Gibbs free energies of dehydration of smectites with monovalent cations in the interlayer sites range from −374 to 1047 cal/mol, and those for their divalent counterparts vary from 4160 to 5842 cal/mol. Owing to the magnitude of these values, it can be deduced that failure to include

explicit provision for interlayer H_2O in equilibrium calculations involving smectites may lead to serious discrepancies between the results of thermodynamic calculations and phase relations observed in nature.

Curves representing equilibrium activities of H_2O as a function of X_{hs} at 25°C and 1 bar are shown in figures 8 and 9 for K-, NH_4-, Rb-, Cs-, Mg-, Sr-, and Ba-smectite dehydration. The curves shown in these figures were generated from eqs (12) and (13) using values of log K and W_s taken from table 3. Calculated values of X_{hs} for $a_{H_2O} = 1$ corresponding to homogeneous equilibrium at 25°C and 1 bar for homoionic K-, Na-, NH_4-, Rb-, Cs-, Ca-, Mg-, Sr-, and Ba-smectite are also given in table 3. It can be deduced from figures 8 and 9 and table 3 that interlayer cations with the same charge and smaller effective electrostatic radii interact to a
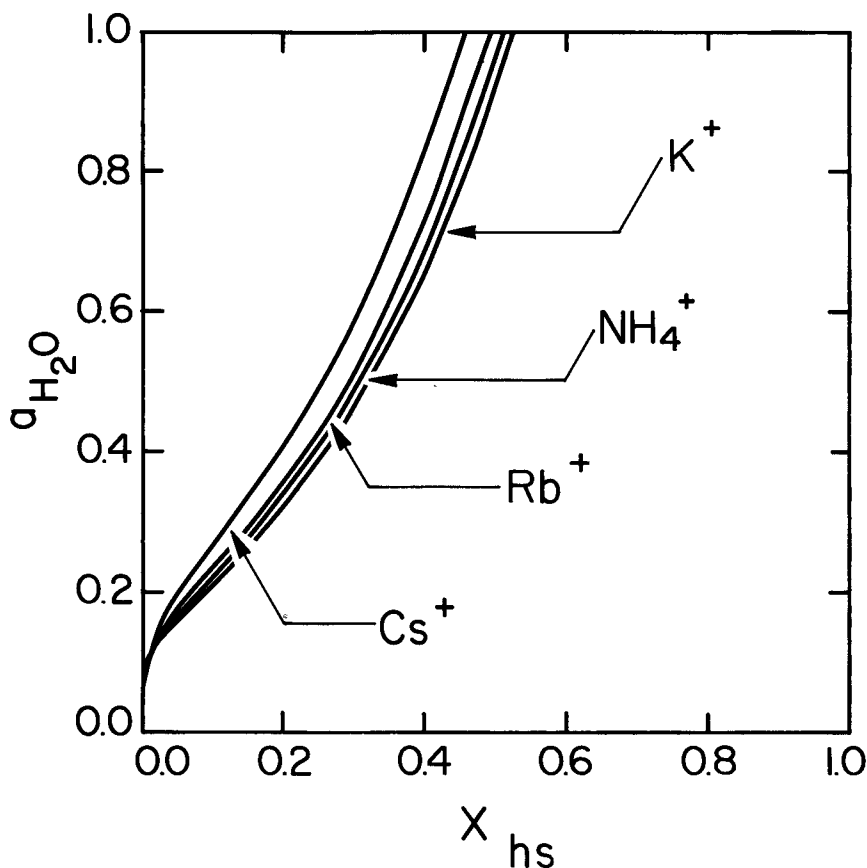
Fig. 8. Equilibrium activity of H_2O as a function of the mole fractions of the hydrous component (X_{hs}) of K-, NH_4-, Rb-, and Cs-smectites at 25°C and 1 bar assuming regular solid solution of homologous hydrous and anhydrous smectite components (see text). The curves were generated from eqs. (12) and (13) using values of W_s and log K taken from table 3.
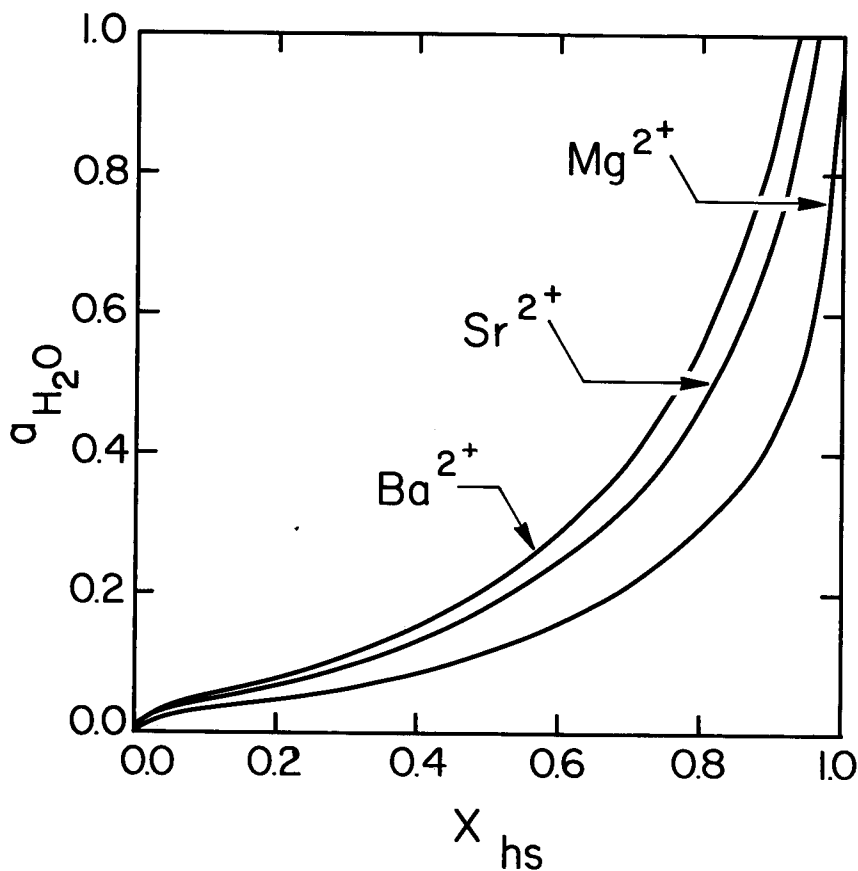
Fig. 9. Equilibrium activity of H_2O as a function of the mole fractions of the hydrous component (X_{hs}) of Mg-, Sr-, and Ba-smectites at 25°C and 1 bar assuming regular solid solution of homologous hydrous and anhydrous smectite components (see text). The curves were generated from eqs (12) and (13) using values of W_s and log K taken from table 3.

greater degree with their associated H_2O dipoles at a given activity of H_2O than those with larger values of $r_{e,j}$. Consequently, the curves in figure 9 for smectites containing divalent interlayer cations occur at higher values of X_{hs} than those for smectites cotaining monovalent interlayer cations. This displacement results from the relative differences in the magnitudes of the solvation energies of cations with different charges.

It can be seen in figures 7 and 9 that at unit activity of H_2O, the values of X_{hs} for Ca-, Mg-, Sr-, and Ba-smectite fall within 0.965 ± 0.025, indicating that solid solutions of hydrous and anhydrous smectite components with divalent cations in the interlayer sites are almost fully hydrated at 25°C and 1 bar. In contrast, the corresponding range of X_{hs} for

smectites containing monovalent cations shown in figures 6 and 8 is 0.53 ± 0.09.

The relative differences in H_2O content at $a_{H_2O} = 1$ for the predicted equilibrium hydration states of the smectite solid solutions shown in figures 6 to 9 correlate well with the H_2O content of smectites immersed in water at 25°C and 1 bar. For example, MacEwan and Wilson (1980) report that K-, NH_4-, and Cs-smectites immersed in water exhibit hydration states that are only about half of those expected for their fully hydrated (~ 15.7 Å) equivalents. This H_2O content is consistent with those at 25°C and 1 bar computed from values of X_{hs} generated for these smectites at $a_{H_2O} = 1$ in the present study (see figs. 6–9). Similarly, basal spacings reported by MacEwan and Wilson (1980) for smectites with divalent cations in the interlayer sites indicate essentially complete hydration of the ~ 5.7 Å interlayers in the mineral at 25°C and 1 bar, which is compatible with the predicted values of X_{hs} shown in figures 7 and 9 for $a_{H_2O} = 1$. The H_2O content of Na-smectites reported by MacEwan and Wilson (1980) is substantially larger than that predicted in the present study. This difference is probably due to the relatively small electrostatic radius of Na^+, which may cause excess sample hydration at activities of H_2O above ~ 0.9.

CORRELATION OF THE REGULAR SOLUTION MODEL WITH X-RAY DATA

As noted above, the regular solution model adopted in the present study requires a random distribution of the hydrous and anhydrous smectite components represented schematically in reaction (2). Although thermodynamic components of minerals do not necessarily have any physical significance, the close agreement of the hydration states predicted in the present study and those observed in natural clay samples indicates that the hydrous and anhydrous components of smectites may well correspond to hydrous and anhydrous layers in the mineral. Provided that the anhydrous layers are not disrupted during sample preparation, they should remain unresponsive to their environment. These samples will then generate X-ray diffraction patterns indicating randomly interstratified mixed layering. This is not to say that all randomly interstratified mixed-layered clay patterns originate in this way. Many no doubt arise from replacement of the mineral smectite by the mineral illite or vice versa. Others probably represent physical mixtures of two or more different layer silicates. Nevertheless, such possibilities are rarely considered in conventional interpretations of X-ray patterns of smectite-bearing samples. In these interpretations, all non-expandable 10Å 2:1 clay layers are labeled as illite, and all expandable interlayers are deemed to be smectite. *despite the fact that K-bearing anhydrous smectite layers have the same d-spacing as illite.* The latter observation, together with others summarized by Ransom and Helgeson (1989, 1993) leave little doubt that the practice of labeling layers with mineral names solely on the basis of XRD is misleading and should be discontinued. Although different techniques of sample preparation appear to have little or no effect on the expandabil-

ity of clay samples (Reynolds, 1992), further development of the environmental TEM and improved sample preparation techniques specifically designed to preserve smectite in its natural hydration state are required before we can achieve a better understanding of the chemistry of the interlayers in this mineral.

<div align="center">CONCLUDING REMARKS</div>

The thermodynamic analysis described above provides a framework for calculating the equilibrium hydration states of smectites and the associated standard molal Gibbs free energies of reaction (2). The calculations indicate that smectites can be regarded as regular solid solutions of hydrous and anhydrous thermodynamic components which differ in composition only by the presence or absence of 4.5 moles of H_2O. Solid solution of these components is probably manifested physically in smectite crystallites by randomly interstratified ~ 15.7Å hydrous and ~ 10Å anhydrous layers which, if undisturbed during sample preparation, should produce XRD patterns similar to those presently attributed to randomly interstratified mixed layer clays. Ordered layering in clay samples will be considered in a subsequent communication (Ransom and Helgeson, in preparation).

The fact that the hydration states of smectite predicted in the present study are in close agreement with those reported in the literature for smectites immersed in water at 25°C and 1 bar strongly supports the generality of the thermodynamic calculations carried out in the present study. These calculations have been extended to include the standard partial molal entropy, volume, heat capacity, and enthalpy of interlayer H_2O, as well as the apparent standard molal Gibbs free energies and enthalpies of reaction at elevated temperatures and pressures of smectite dehydration during sediment burial and diagenesis (Ransom and Helgeson, 1994a, b).

I am more than grateful to you for patiently sharing your brilliance and extending to me your warm friendship and support through the years. May it continue for many more!

APPENDIX A

Ideal solid solution representation of smectite dehydration

The law of mass action represented by reaction (2) for ideal binary solid solutions of homologous hydrous and anhydrous smectite components can be written as

$$K = \frac{X_{as} a_{H_2O}^{n_c}}{X_{hs}} \tag{A.1}$$

where K designates the equilibrium constant for the reaction, X_{hs} and X_{as} represent the mole fractions of the hydrous and anhydrous components of the solid solution, respectively, a_{H_2O} denotes the activity of H_2O in the aqueous phase, and n_c refers to the stoichiometric number of moles of H_2O in the hydrous smectite component. Restating eq (A.1) in terms of its logarithmic analog and combining the result with eq (7) leads to

$$\log a_{H_2O} = -\frac{1}{n_c} \log \left(\frac{1 - X_{hs}}{X_{hs}} \right) + \frac{\log K}{n_c}. \tag{A.2}$$

It follows from this expression and eq (15) that homogenous equilibrium in an ideal binary solid solution of homologous hydrous and anhydrous smectite components requires $\log a_{H_2O}$ to be a linear function of $\log ((1 - X_{hs})/X_{hs})$ with a slope of $-1/4.5$ and an intercept of $\log K/4.5$.

Values of $\log ((1 - X_{hs})/X_{hs})$ were computed from eqs (16) and (17) as a function of $\log a_{H_2O}$ using the smectite water-vapor pressure isotherm data for Na- and Ca-smectite reported by Keren and Shainberg (1975). These values are plotted in figures A.1 and A.2 as
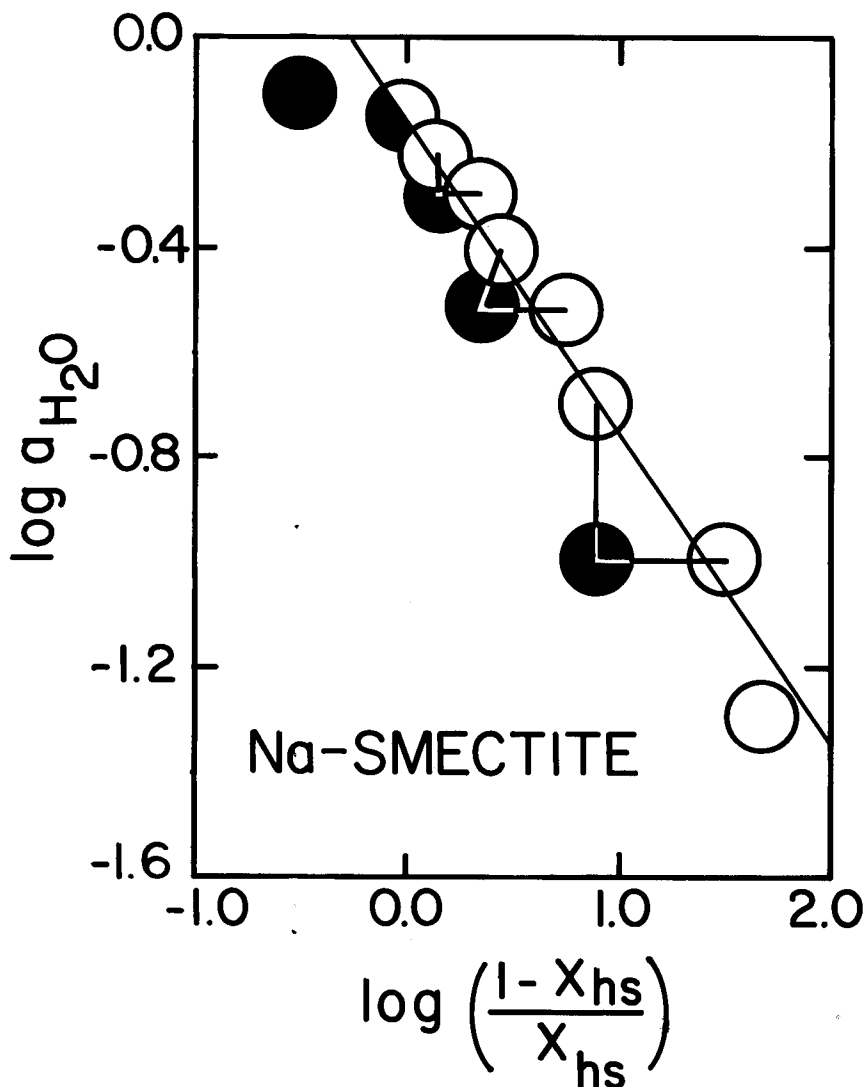
Fig. A.1. Log a_{H_2O} at 25°C and 1 bar as a function of log $((1 - X_{hs})/X_{hs})$ computed from Na-smectite water-vapor pressure isotherm data assuming ideal solid solubility of hydrous and anhydrous Na-smectite components. The white and black circles represent hydration and dehydration isotherms, respectively, reported by Keren and Shainberg (1975). The half white and half black symbols and the white and black circles connected by short straight lines bracket the equilibrium smectite composition.

black and white circles, which represent smectite hydration and dehydration, respectively. The symbols corresponding to data that bracket equilibrium values of log $((1 - X_{hs})/X_{hs})$ and log a_{H_2O} are shown in these figures as half black and half white circles or black and white° circles connected by short straight lines. The lines drawn through the symbols in the figures
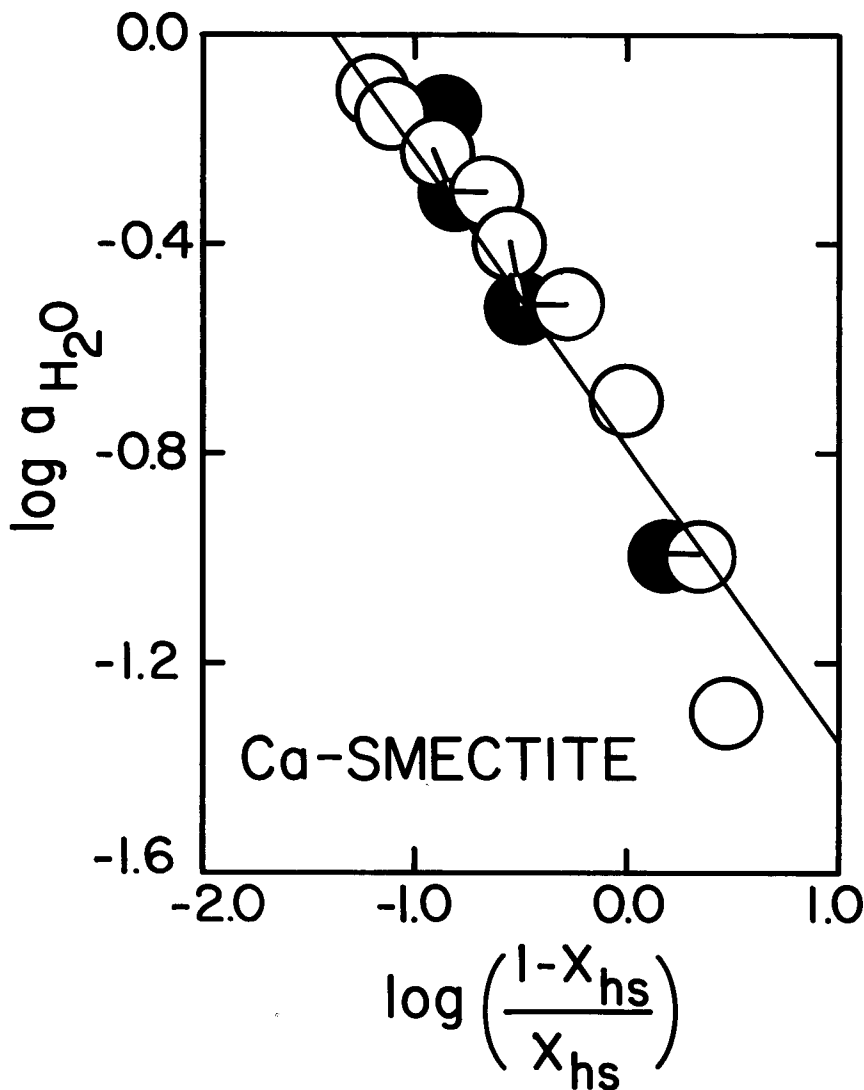
Fig. A.2. Log a_{H_2O} at 25°C and 1 bar as a function of log $((1 - X_{hs})/X_{hs})$ computed from Ca-smectite water-vapor pressure isotherm data assuming ideal solid solubility of hydrous and anhydrous Ca-smectite components (see caption of fig. A.1).

represent graphical fits of the data with the least negative slopes permitted by the distribution of the equilibrium brackets. The slopes of these lines are −0.55 for Na-smectite (fig. A.1) and −0.58 for Ca-smectite (fig. A.2), both of which differ substantially from the −1/4.5 (that is, −0.22) slope required by eq (A.2) for ideal solution behavior. Hence, Na- and Ca-smectite cannot be regarded as ideal solid solutions of homologous hydrous and

anhydrous components. It can be shown that the same observation applies also to ideal site mixing of H_2O dipoles and vacancies in the interlayer sites.

<div align="center">APPENDIX B</div>

Relative humidities and the activity of H_2O referenced to the liquid standard state

The relative humidity ($p_{H_2O}/p_{H_2O}^\circ$) is equal to the partial pressure of H_2O in the vapor (p_{H_2O}) divided by the partial pressure of H_2O corresponding to the equilibrium solubility of water in the vapor phase ($p_{H_2O}^\circ$) at the pressure and temperature of interest. The relation between relative humidity and the activity of H_2O can be described by taking account of equilibrium between H_2O in an aqueous solution and that in a coexisting gas phase, which can be expressed as

$$H_2O \rightleftarrows H_2O_{(g)} \qquad (B.1)$$

where H_2O and $H_2O_{(g)}$ stand for H_2O in the liquid and gas phases, respectively. The law of mass action for reaction (B.1) can be written as

$$K = \frac{f_{H_2O}}{a_{H_2O}} \qquad (B.2)$$

where K represents the equilibrium constant for reaction (B.1), f_{H_2O} designates the fugacity of H_2O vapor, and a_{H_2O} refers to the activity of H_2O in the liquid phase. The fugacity of H_2O can be expressed as

$$f_{H_2O} = \chi_{H_2O} p_{H_2O} \qquad (B.3)$$

where χ_{H_2O} stands for the fugacity coefficient of H_2O vapor at the temperature and pressure of interest. Combining eqs (B.2) and (B.3) leads to

$$K = \frac{\chi_{H_2O} p_{H_2O}}{a_{H_2O}}. \qquad (B.4)$$

Because χ_{H_2O} in air at 25°C and 1 bar is essentially unity (Belonoshko, Shi, and Saxena, 1992), eq (B.4) can be written in a close approximation as

$$a_{H_2O} \approx \frac{p_{H_2O}}{K}. \qquad (B.5)$$

The equilibrium constant K can be expressed in terms of the standard molal Gibbs free energy of formation from the elements of water ($\Delta G_{f,H_2O}^\circ$) and steam ($\Delta G_{f,H_2O_{(g)}}^\circ$) by writing

$$K = \exp\left(\frac{\Delta G_{f,H_2O}^\circ - \Delta G_{f,H_2O_{(g)}}^\circ}{RT}\right) \qquad (B.6)$$

where R refers to the gas constant, and T represents the temperature in Kelvins. Taking values for $\Delta G_{f,H_2O}^\circ$ and $\Delta G_{f,H_2O_{(g)}}^\circ$ at 25°C and 1 bar from Wagman and others (1982), which are compatible with the standard states adopted in the present study (see footnote 3), leads to $K = 0.0316$. This values corresponds to $p_{H_2O}^\circ$, which is given by Weast, Astle, and Beyer (1987) as 0.03167 bars at 25°C and 1 bar. The relation between the activity of H_2O in the liquid state and the relative humidity can thus be expressed as

$$a_{H_2O} \approx \frac{p_{H_2O}}{p_{H_2O}^\circ}. \qquad (B.7)$$

REFERENCES

Bailey, S. W., 1980, Structures of layer silicates, *in* Brindley, G. W., and Brown, G., editors, Crystal Structures of Clay Minerals and their X-ray Identification: London, Mineralogical Society, p. 1–123.

Bangham, D. H., 1944, Thermodynamics of sorption isotherms: The hysteresis loop in capillary condensation: London, Nature, v. 154, p. 837–838.

Barshad, Isaac, 1955, Adsorption and swelling properties of clay-water systems: Bulletin of the California Department of Natural Resources Division of Mines, v. 169, p. 90–177.

———— 1960, Thermodynamics of water adsorption and desorption on montmorillonite, *in* Swineford, Ada, and Frank, P. C., editors, Clay & Clay Minerals, Proceedings of the 8th National Clay Conference, 1959, Norman, Oklahoma: New York, Pergamon Press, p. 84–101.

Belonoshko, A. B., Shi, P., and Saxena, S. K., 1992, Superfluid: A Fortran-77 program for calculation of Gibbs free energy and volume of C-H-O-N-S-Ar mixtures: Computers and Geoscience, v. 18, p. 1267–1269.

Berman, R. G., and Brown, T. H., 1985, Heat capacity of minerals in the system Na_2O-K_2O-CaO-MgO-FeO-Fe_2O_3-Al_2O_3-SiO_2-TiO_2-H_2O-CO_2 representation, estimation, and high temperature extrapolation: Contributions to Mineralogy and Petrology, v. 89, p. 168–183.

Bird, Peter, 1984, Hydration-phase diagrams and friction of montmorillonite under laboratory and geologic conditions with implications for shale compaction, slope instability, and strength of fault gouge: Tectonophysics, v. 107, p. 235–260.

Bjerrum, N., 1929, Neuere Anschauungen über Elektrolyte: Berichte der Deutschen Chemischen Gesellschaft, v. 62, p. 1091–1103.

Born, V. M., 1920, Volumen und Hydratationswarme der Ionen: Zeitschrift für Physik, v. 1, p. 45–48.

Bransom, Kathy, and Newman, A. C. D., 1983, Water sorption on Ca-saturated clays I. Multilayer sorption and microscopy in some illites: Clay Minerals, v. 18, p. 277–287.

Bruce, C. H., 1984, Smectite dehydration-Its relation to structural development and hydrocarbon accumulation in northern Gulf of Mexico basin: American Association of Petroleum Geologists Bulletin, v. 68, p. 673–683.

Burst, J. F., 1969, Diagenesis of Gulf Coast clayey sediments and its possible relation to petroleum migration: American Association of Petroleum Geologists Bulletin, v. 53, p. 73–93.

Chermak, J. A. and Rimstidt, J. D., 1989, Estimating the thermodynamic properties (ΔG_f^o and ΔH_f^o) of silicate minerals at 298 K from the sum of polyhedral contributions: American Mineralogist, v. 74, p. 1023–1031.

Colten, V. A., 1986, Hydration states of smectite in NaCl brines at elevated pressures and temperatures: Clays & Clay Minerals, v. 34, p. 385–389.

Davidtz, J. C., and Lowe, P. F., 1970, Relation between crystal-lattice configuration and swelling of montmorillonites: Clays & Clay Minerals, v. 18, p. 325–332.

Delon, J. F., Lietard, J. M., Cases, J. M., and Yvon, J., 1986, Determination of porosity of platey materials using slit-shaped and beveled pores: Clay Minerals, v. 21, p. 361–375.

Eberl, D. D., Srodon, J., and Northrop, H. R., 1986, Potassium fixation in smectite by wetting and drying, *in* Davis, J. A., and Hayes, K. F., editors, Geochemical Processes at Mineral Surfaces: Washington, D.C., American Chemical Society, p. 296–326.

Foster, M. D., 1953, Geochemical studies of clay minerals II-Relation between ionic substitution and swelling in montmorillonites: American Mineralogist, v. 38, p. 994–1006.

———— 1955, The relation between composition and swelling in clays: Clays & Clay Minerals, v. 3, p. 205–220.

Fripiat, J. J., Jelli, A., Poncelet, G., and Andre, J., 1965, Thermodynamic properties of adsorbed water molecules and electrical conduction in montmorillonites and silicates: Journal of Physical Chemistry, v. 69, p. 2185–2197.

Glaser, Rachel, and Mering, M. J., 1968, Domaines d'hydration homogénée des smectites: Compte Rendu Academie de Science Paris, Series D, v. 267, p. 463–466.

Greene-Kelley, R., 1962, Charge densities and heats of immersion of some clay minerals: Clay Minerals Bulletin, v. 5, p. 1–8.

Gregg, S. J., and Sing, K. S. W., 1967, Adsorption, Surface Area and Porosity: New York, Academic Press, 371 p.

Hall, P. L., 1981, Neutron scattering techniques for the study of clay minerals, *in* Fripiat, J. J., editor, Advanced Techniques for Clay Mineral Analysis: Amsterdam, Elsevier, p. 51–75.

Hall, P. L., and Astill, D. M., 1989, Adsorption of water by homoionic exchange forms of Wyoming montmorillonite SWy-1: Clays & Clay Minerals, v. 37, p. 335–363.

Hall, P. L., Astill, D. M., and McConnell, J. D. C., 1986, Thermodynamic and structural aspects of the dehydration of smectites in sedimentary rocks: Clay Minerals, v. 21, p. 633–648.

Hawkins, R. K., and Egelstaff, P. A., 1980, Interfacial water structure in montmorillonite from neutron diffraction experiments: Clays & Clay Minerals, v. 28, p. 19–20.

Helgeson, H. C., Delany, J. M., Nesbitt, W. H., and Bird, D. K., 1978, Summary and critique of the thermodynamic properties of rock-forming minerals: American Journal of Science, v. 278-A, p. 1–229.

Helgeson, H. C., Kirkham, D. H., and Flowers, G. C., 1981, Theoretical prediction of the thermodynamic behavior of aqueous electrolytes at high pressures and temperatures: IV. Calculation of activity coefficients, osmotic coefficients, and apparent molal and standard and relative partial molal properties to 600°C and 5 kb: American Journal of Science, v. 281, p. 1249–1516.

Johansen, R. T., and Dunning, H. N., 1959, Water-vapor adsorption on clays: Clays & Clay Minerals, v. 23, p. 249–258.

Keenan, A. G., Mooney, R. W., and Wood, L. A., 1951, The relation between exchangeable ions and water sorption on kaolinite: Journal of Physical and Colloidal Chemistry, v. 55, p. 1462–1473.

Keren, R., and Shainberg, I., 1975, Water vapor isotherms and heat of immersion of Na/Ca-montmorillonite systems—I: Homoionic clay: Clays & Clay Minerals, v. 23, p. 193–200.

————— 1979, Water vapor isotherms and heat of immersion of Na/Ca-montmorillonite systems—II: Mixed systems: Clays & Clay Minerals, v. 27, p. 145–151.

————— 1980, Water-vapor isotherms and heat of immersion of Na- and Ca-montmorillonite systems III: Thermodynamics: Clays & Clay Minerals, v. 28, p. 204–210.

Khitarov, N. I., and Pugin, V. A., 1966, Behavior of montmorillonite under elevated temperatures and pressures: Geokhimiya, v. 7, p. 790–795.

Koster van Groos, A. F., and Guggenheim, S., 1984, The effect of pressure on the dehydration reaction of interlayer water in Na-montmorillonite: American Mineralogist, v. 69, p. 872–879.

————— 1986, Dehydration of K-exchanged montmorillonite at elevated temperatures and pressures: Clays & Clay Minerals, v. 34, p. 281–286.

————— 1987, Dehydration of a Ca- and Mg-exchanged montmorillonite SWy-1 at elevated pressures: American Mineralogist, v. 72, p. 259–278.

Kraehenbuehl, F., Stoeckli, H. F., Brunner, F., Kahr, G., and Mueller-Vonmoos, M., 1987, Study of the water-bentonite system by vapor adsorption, immersion calorimetry and X-ray techniques: I. Micropore volumes and internal surface areas, following Dubinin's theory: Clay Minerals, v. 22, p. 1–9.

Lecloux, A., and Pirard, J. P., 1979, The importance of standard isotherms in the analysis of adsorption isotherms for determining the porous texture of solids: Journal of Colloidal Interface Science, v. 70, p. 265–281.

MacEwan, D. M. C., and Wilson, M. J., 1980, Interlayer and intercalation complexes of clay minerals, *in* Brindley, G. W., and Brown, G., editors, Crystal Structures of Clay Minerals and their X-ray Identification: London, Mineralogical Society, p. 197–248.

Martin, T. R., 1959, Water-vapor sorption on kaolinite: Hysteresis: Clays & Clay Minerals, v. 2, p. 259–278.

————— 1962, Adsorbed water on clay: A review, *in* Swineford, Ada, and Franks, P. C., editors, Proceedings of the 9th National Conference on Clays and Clay Minerals: New York, Pergamonon Press, p. 23–70.

Mason, Geoffrey, 1982, The effect of pore space connectivity on the hysteresis of capillary condensation in adsorption-desorption isotherms: Journal of Colloid and Interface Science, v. 88, p. 36–46.

Mathieson, A. M., and Walker, G. F., 1954, Crystal structure of magnesium-vermiculite: American Mineralogist, v. 39, p. 321–255.

Mattigod, S. V., and Sposito, G., 1978, Improved method for estimating the standard free energies of formation for smectites: Geochemica et Cosmochimica Acta. v. 42, p. 1753–1762.

Mooney, R. W., Keenan, A. G., and Wood, L. A., 1952, Adsorption of water vapor by montmorillonite. I. Heat of desorption and application of BET theory: Journal of the American Chemical Society, v. 74, p. 1367–1371.

Newman, A. C. D., 1987, The interaction of water with clay mineral surfaces, *in* Newman, A. C. D., editor, Chemistry of Clays and Clay Minerals: New York, John Wiley & Sons, p. 237–274.

Newman, A. C. D., and Brown, G., 1987, The chemical constitution of clays, *in* Newman, A. C. D., editor, Chemistry of Clays and Clay Minerals: New York, John Wiley & Sons, p. 1–128.

Newton, R. C., 1987, Thermodynamic analysis of phase equilibria in simple mineral systems, *in* Carmichael, I. S. E., and Eugster, H. P., editors, Thermodynamic Modeling of Geologic Materials: Minerals, Fluids, and Melts: Chelsea, Michigan, Bookcrafters, Inc., Mineralogical Society of America, p. 1–34.

Nriagu, Jerome, 1975, Thermochemical approximations for clay minerals: American Mineralogist, v. 60, p. 834–839.

Omerod, E. C., and Newman, A. C. D., 1983, Water sorption on Ca-saturated clays: II. Internal and external surfaces of montmorillonite: Clay Minerals, v. 18, p. 289–299.

Perry, E. A., and Hower, J., 1972, Late-stage dehydration in deeply buried sediments: American Association of Petroleum Geologists Bulletin, v. 56, p. 2013–2021.

Powers, M. C., 1967, Fluid release mechanisms in compacting marine mudrocks and their importance in oil exploration: American Association of Petroleum Geologists Bulletin, v. 51, p. 1240–1254.

Ransom, Barbara, and Helgeson, H. C., 1989, On the correlation of expandability with mineralogy and layering in mixed-layer clays: Clays & Clay Minerals, v. 37, p. 189–191.

———— 1993, Compositional end members and thermodynamic components of illite and dioctahedral aluminous smectite solid solutions: Clays & Clay Minerals, v. 41, p. 537–550.

———— 1994a, A chemical and thermodynamic model of dioctahedral 2:1 layer clay minerals in diagenetic processes: Interlayer dehydration of smectite as a function of temperature and depth in sedimentary basins: American Journal of Science, (in press).

———— 1994b, Estimation of the molal heat capacities, entropies, and volumes of 2:1 clay minerals: Geochimica et Cosmochimica Acta, in press.

———— 1994c, A crystallochemical and structural model of the formation and constitution of randomly interstratified mixed-layer clays (in preparation).

Rao, C. N. R., 1972, Theory of hydrogen bonding in water, *in* Franks, F., editor, Water, A Comprehensive Treatise: New York, Plenum Press, p. 93–114.

Reynolds, R. C., 1992, X-ray diffraction studies of illite/smectite from rocks: <1 μm randomly oriented powders and <1 μm oriented powder aggregates: The absence of laboratory artifacts: Clays & Clay Minerals, v. 40, p. 387–398.

Rieke, H. H., and Chilingarian, G. V., 1974, Compaction of Argillaceous Sediments: New York, Elsevier, 424 p.

Roderick, G. L., Senich, D., and Demirel, T., 1969, X-ray diffraction studies of the montmorillonite-water system, *in* Heller, L., editor, Proceedings of the International Clay Conference, Tokyo: Jerusalem, Israel, Universities Press, p. 659–668.

Schultz, L. G., 1969, Lithium and potassium absorption, dehydroxylation temperature and structural water content of aluminous smectites: Clays & Clay Minerals, v. 19, p. 137–150.

Shock, Everett L., and Helgeson, H. C., 1988, Calculation of the thermodynamic and transport properties of aqueous species at high pressures and temperatures: Correlation algorithms for ionic species and equation of state predictions to 5 kb and 1000°C: Geochimica et Cosmochimica Acta, v. 52, p. 2009–2036.

Sposito, Garrison, and Prost, R., 1982, Structure of water adsorbed on smectites: Chemistry Review, v. 82, p. 553–573.

Suquet, Helène, de la Calle, C., and Pezerat, H., 1975, Swelling and structural organization of saponite: Clays & Clay Minerals, v. 23, p. 1–9.

Tardy, Yves, and Duplay, J., 1992, A method of estimating the Gibbs free energies of formation of hydrated and dehydrated clay minerals: Geochimica et Cosmochimica Acta, v. 56, p. 3007–3029.

Tardy, Yves, and Garrels, R. M., 1974, A method of estimating Gibbs energies of formation of layer silicates: Geochimica et Cosmochimica Acta, v. 38, p. 1101–1116.

Tardy, Yves, Lesniak, P., Duplay, J., and Prost, R., 1980, Energies d'hydration des argiles: Application à l'hectorite: Bulletin Mineralogique, v. 103, p. 217–223.

Tardy, Yves, and Touret, O., 1987, Hydration energies of smectite: A model for glauconite, illite, and corrensite formation, *in* Schultz, L. G., van Olphen, H., and Mumpton, F. A., editors, Proceedings of the International Clay Conference, Denver, 1985: Bloomington, Indiana, The Clay Minerals Society, p. 46–52.

van Olphen, H., 1963, Compaction of clay sediments in the range of molecular particle distances, Proceedings of the 11th National Conference on Clays and Clay Minerals: Washington, D.C., National Academy of Sciences, National Research Council, p. 178–187.

———— 1965, Thermodynamics of interlayer adsorption of water in clays: I. Sodium vermiculite: Journal of Colloid Science, v. 20, p. 822–837.

Wagman, D. D., Evans, W. H., Parker, V. B., Schumm, R. H., Halow, I., Bailey, S. M., Churney, K. L., and Nuttall, R. L., 1982, The NBS tables of chemical thermodynamic properties. Selected values for inorganic and C_1 and C_2 organic substances in SI units: Journal of Physical Chemistry Reference Data, v. 11, Supplement 2, p. 1–392.

Weast, R. C., Astle, M. J., and Beyer, W. H., 1987, CRC Handbook of Chemistry and Physics: Boca Raton, Florida, CRC Press Inc.

Weaver, C. E., and Pollard, L. D., 1973, The Chemistry of Clay Minerals: New York, Elsevier, 213 p.